Sagar, M., Wu, X., Lee, S., Overbaugh, J., 2006. Human immunodeficiency virus type 1 V1-V2 envelope loop sequences expand and add glycosylation sites over the course of infection, and these modifications affect antibody neutralization sensitivity. J. Virol. 80 (19), 9586–9598.

Shibata, R., Kawamura, M., Sakai, H., Hayami, M., Ishimoto, A., Adachi, A., 1991. Generation of a chimeric human and simian immunodeficiency virus infectious to monkey peripheral blood mononuclear cells. J. Virol. 65 (7), 3514–3520.

Shimizu, Y., Okoba, M., Yamazaki, N., Goto, Y., Miura, T., Hayami, M., Hoshino, H., Haga, T., 2006. Construction and in vitro characterization of a chimeric simian and human immunodeficiency virus with the RANTES gene. Microbes. Infect. 8 (1), 105–113.

Shinohara, K., Sakai, K., Ando, S., Ami, Y., Yoshino, N., Takahashi, E., Someya, K., Suzaki, Y., Nakasone, T., Sasaki, Y., Kaizu, M., Lu, Y., Honda, M., 1999. A highly pathogenic simian/human immunodeficiency virus with genetic changes in cynomolgus monkey. J. Gen. Virol. 80, 1231–1240.

Shiver, J.W., Fu, T.M., Chen, L., Casimiro, D.R., Davies, M.E., Evans, R.K., Zhang, Z.Q., Simon, A.J., Trigona, W.L., Dubey, S.A., Huang, L., Harris, V.A., Long, R.S., Liang, X., Handt, L., Schleif, W.A., Zhu, L., Freed, D.C., Persaud, N.V., Guan, L., Punt, K.S., Tang, A., Chen, M., Wilson, K.A., Collins, K.B., Heidecker, G.J., Fernandez, V.R., Perry, H.C., Joyce, J.G., Grimm, K.M., Cook, J.C., Keller, P.M., Kresock, D.S., Mach, H., Troutman, R.D., Isopi, L.A., Williams, D.M., Xu, Z., Bohannon, K.E., Volkin, D.B., Montefiori, D.C., Miura, A., Krivulka, G.R., Lifton, M.A., Kuroda, M.J., Schmitz, J.E., Letvin, N.L., Caulfield, M.J., Bett, A.J., Youil, R., Kaslow, D.C., Emini, E.A., 2002. Replication-incompetent adenoviral vaccine vector elicits effective anti-immunodeficiency-virus immunity. Nature 415 (6869), 331–335.

Sing, T., Low, A.J., Beerenwinkel, N., Sander, O., Cheung, P.K., Domingues, F.S., Büch, J., Däumer, M., Kaiser, R., Lengauer, T., Harrigan, P.R., 2007. Predicting HIV coreceptor usage on the basis of genetic and clinical covariates. Antivir. Ther. 12 (7), 1097–1106.

Tan, R.C., Harouse, J.M., Gettie, A., Cheng-Mayer, C., 1999. In vivo adaptation of SHIV (SF162): chimeric virus expressing a NSI, CCR5-specific envelope protein. J. Med. Primatol. 28 (4-5), 164–168.

Trkola, A., Kuhmann, S.E., Strizki, J.M., Maxwell, E., Ketas, T., Morgan, T., Pugach, P., Xu, S., Wojcik, L., Tagat, J., Palani, A., Shapiro, S., Clader, J.W., McCombie, S., Reyes, G.R., Baroudy, B.M., Moore, J.P., 2002. HIV-1 escape from a small molecule, CCR5-specific entry inhibitor does not involve CXCR4 use. Proc. Natl. Acad. Sci. U.S.A. 99, 395–400.

Veazey, R.S., DeMaria, M., Chalifoux, L.V., Shvetz, D.E., Pauley, D.R., Knight, H.L., Rosenzweig, M., Johnson, R.P., Desrosiers, R.C., Lackner, A.A., 1998. Gastrointestinal tract as a major site of CD4+ T cell depletion and viral replication in SIV infection. Science 280 (5362), 427–431.

Wei, X., Decker, J.M., Wang, S., Hui, H., Kappes, J.C., Wu, X., Salazar-Gonzalez, J.F., Salazar, M.G., Kilby, J.M., Saag, M.S., Komarova, N.L., Nowak, M.A., Hahn, B.H., Kwong, P.D., Shaw, G.M., 2003. Antibody neutralization and escape by HIV-1. Nature 422 (6929), 307–312.

Willey, R.L., Smith, D.H., Lasky, L.A., Theodore, T.S., Earl, P.L., Moss, B., Capon, D.J., Martin, M.A., 1988. In vitro mutagenesis identifies a region within the envelope gene of the human immunodeficiency virus that is critical for infectivity. J. Virol. 62 (1), 139–147.

Yamaguchi-Kabata, Y., Yamashita, M., Ohkura, S., Hayami, M., Miura, T., 2004. Linkage of amino acid variation and evolution of human immunodeficiency virus type 1 gp120 envelope glycoprotein (subtype B) with usage of the second receptor. J. Mol. Evol. 58 (3), 333–340.

Zhang, Y., Lou, B., Lal, R.B., Gettie, A., Marx, P.A., Moore, J.P., 2000. Use of inhibitors to evaluate coreceptor usage by simian and simian/human immunodeficiency viruses and human immunodeficiency virus type 2 in primary cells. J. Virol. 74 (15), 6893–6910.

Web references

Web PSSM, Mullins Lab, University of Washington http://indra.mullins.microbiol.washington.edu/webpssm/

Geno2pheno [coreceptor], Max-Planck-Institut Informatik. http://coreceptor.bioinf.mpi-inf.mpg.de

Vaccine 28 (2010) 5377–5385

Contents lists available at ScienceDirect

Vaccine

journal homepage: www.elsevier.com/locate/vaccine

Evaluation of the immune response and protective effects of rhesus macaques vaccinated with biodegradable nanoparticles carrying gp120 of human immunodeficiency virus

Ai Himeno[a], Takami Akagi[b,d], Tomofumi Uto[c,d], Xin Wang[c,d], Masanori Baba[c,d], Kentaro Ibuki[a], Megumi Matsuyama[a], Mariko Horiike[a], Tatsuhiko Igarashi[a], Tomoyuki Miura[a,d,*], Mitsuru Akashi[b,d,**]

[a] Laboratory of Primate Model, Experimental Research Center for Infectious Diseases, Institute for Virus Research, Kyoto University, 53 Shogoinkawaramachi, Sakyo-ku, Kyoto 606-8507, Japan

[b] Department of Applied Chemistry, Graduate School of Engineering, Osaka University, 2-1 Yamadaoka, Suita, Osaka 565-0871, Japan

[c] Division of Antiviral Chemotherapy, Center for Chronic Viral Diseases, Graduate School of Medical and Dental Sciences, Kagoshima University, 8-35-1 Sakuragaoka, Kagoshima 890-8544, Japan

[d] Japan Science and Technology Agency (JST), Core Research for Evolutional Science and Technology (CREST), Saitama 332-0012, Japan

ARTICLE INFO

Article history:
Received 26 January 2010
Received in revised form 6 April 2010
Accepted 15 April 2010
Available online 14 May 2010

Keywords:
HIV vaccine
Biodegradable nanoparticles
Adjuvant

ABSTRACT

We previously reported that biodegradable amphiphilic poly(γ-glutamic acid) nanoparticles (NPs) carrying the recombinant gp120 env protein of the human immunodeficiency virus type 1 (HIV-1) were efficiently taken up by dendritic cells, and induced strong $CD8^+$ T cell responses against the gp120 in mice. To evaluate gp120-carrying NPs (gp120-NPs) as a vaccine candidate for HIV-1 infection, we vaccinated rhesus macaques with these gp120-NPs and examined the immune response and protective efficacy against a challenge inoculation of simian and human immunodeficiency chimeric virus (SHIV). We found that gp120-NP vaccination induced stronger responses for both gp120-specific cellular and humoral immunity than gp120-alone vaccination. After the challenge inoculation with SHIV, however, the peak value of viral RNA in the peripheral blood was higher in the vaccinated groups, especially the gp120-NP vaccinated group, than naive control group. Higher value of viral load was also maintained in gp120-NP vaccinated group. Furthermore, $CD4^+$ T cells from the peripheral blood decreased more in the vaccinated groups than the control group. Thus, induced immune responses against gp120 enclosed in NPs were not effective for protection but, conversely enhanced the infection, although the gp120-NPs showed a stronger induction of immune responses against the vaccinated antigen in rhesus macaques. These results support the importance of determining immune correlate of protective immunity for vaccine development against HIV-1 infection.

1. Introduction

The development of a human immunodeficiency virus type 1 (HIV-1) vaccine is much needed to prevent the continuing spread of the acquired immunodeficiency syndrome (AIDS) pandemic across the world [1]. The use of highly active antiretroviral therapy (HAART) has achieved a reduced death rate due to AIDS. HAART can efficiently suppress virus replication in HIV-1-infected individuals [2]. However, HAART is expensive, and the complete eradication of the virus from infected patients by HAART does not seem possible, suggesting the necessity for long-term treatment. Moreover, the side effects and emergence of drug resistant viruses limit the long-term application of HAART [3]. Thus, an effective, safe and affordable HIV-1 vaccine with prophylactic/therapeutic effects is the most desirable for the eradication of HIV-1 infection.

Vaccination to induce an adaptive immune response is expected for a broad range of infectious diseases. Traditional vaccines are mainly composed of live attenuated viruses or whole inactivated pathogens, and these vaccines often cause many unwanted side effects [4]. With recent advances in biotechnology, new vaccine strategies have been developed using part of the pathogen, such as recombinant/synthetic proteins or peptides, or DNA encoding for these proteins. Subunit vaccines are generally very safe, with well-defined components. However, these antigens are often

* Corresponding author at: Laboratory of Primate Model, Experimental Research Center for Infectious Diseases, Institute for Virus Research, Kyoto University, 53 Shogoinkawaramachi, Sakyo-ku, Kyoto 606-8507, Japan. Tel.: +81 75 751 3984; fax: +81 75 761 9335.

** Corresponding author at: Department of Applied Chemistry, Graduate School of Engineering, Osaka University, 2-1 Yamadaoka, Suita 565-0871, Japan. Tel.: +81 6 6879 7356; fax: +81 6 6879 7359.

E-mail addresses: tmiura@virus.kyoto-u.ac.jp (T. Miura), akashi@chem.eng.osaka-u.ac.jp (M. Akashi).

0264-410X/$ – see front matter © 2010 Elsevier Ltd. All rights reserved.
doi:10.1016/j.vaccine.2010.04.110

poorly immunogenic, and thus require the use of adjuvants or vaccine delivery systems to induce adequate immunity [5–7]. Particulate adjuvants (e.g. micro/nanoparticles, emulsions, ISCOMS, liposomes, virosomes and virus-like particles) have been widely investigated in HIV vaccine delivery systems [8]. Antigen uptake by antigen presenting cells (APCs) is enhanced by the association of these antigens with nano-sized particles. The adjuvant effect of the nanoparticles appears to be largely a consequence of their uptake into the APCs. Dendritic cells (DCs) are highly specialized APCs that can activate naive T cells, and hence initiate primary immune responses. Therefore, the active delivery of antigens to DCs is an important factor for the development of effective vaccines [9,10].

Vaccines to prevent HIV infection have focused on the induction of virus-specific neutralizing antibodies and cytotoxic T lymphocyte (CTL) responses. An important role of neutralizing antibodies for HIV-1 *env* has been demonstrated by the passive transfer of these neutralizing antibodies in animal models. The passive transfer of various human monoclonal antibodies can protect against viral challenge [11–13]. However, it should be noted that for the protection of viral transmission, a high-titer and an enormous quantity of antibodies are needed. Similarly, HIV-1-specific CTL responses have also been associated with the control of HIV-1 infection. The importance of CTL for HIV-1 infection is suggested by the inverse correlation between anti-HIV-1 CTL responses and the virus load in humans [14,15]. In addition, the depletion of $CD8^+$ T cells through the infusion of anti-CD8 antibodies decreases the control of viremia in infected macaques [16,17]. Therefore, recent vaccine approaches have focused on eliciting CTL responses [18]. To solve the problem of the poor immunogenicity of HIV-1 *env*, several candidate adjuvants and delivery systems are currently being investigated in rhesus macaques [19–22]. In fact, the first phase III trial performed using the HIV-1 gp120-based vaccine candidate AIDSVAX from VaxGen was a failure [23]. Varying degrees of protection have been demonstrated in a number of vaccine trials employing the use of a pathogenic simian immunodeficiency virus (SIV) or a chimeric simian/human immunodeficiency virus (SHIV) as the challenge virus [24].

In previous studies, we demonstrated that intranasal immunization with inactivated HIV- or SHIV-capturing polystyrene nanospheres (HIV-NS or SHIV-NS) could induce vaginal anti-HIV-1 gp120 IgA and IgG antibodies in mice [25–27] and macaques, and that SHIV-NS-immunized macaques exhibited partial protection when vaginally and systemically challenged with pathogenic viruses [28]. These results clearly indicated that HIV-1-capturing nanospheres are useful as adjuvant carriers for a prophylactic vaccine against HIV-1 infection. However, both biodegradability and biocompatibility of the adjuvant carriers are required for medical use. Therefore, the development of biodegradable nanoparticles is indispensable for clinical applications [29]. To that end, we have recently prepared protein-loaded biodegradable nanoparticles composed of hydrophobically modified poly(γ-glutamic acid) (γ-PGA) [30–33]. γ-PGA is a naturally occurring water-soluble, biodegradable, edible and non-toxic poly(amino acid)s that is synthesized by certain strains of *Bacillus*. γ-PGA hydrophobic derivatives (γ-hPGA) formed 200 nm-sized nanoparticles (NPs) in water. These protein-encapsulated γ-hPGA NPs were efficiently taken up by immature mouse DCs. These γ-hPGA NPs also had adjuvant activity for DC maturation. Thus, γ-hPGA NPs have significant potential as an antigen carrier and as an adjuvant for DCs [34,35]. Moreover, immunization with HIV-1 gp120- or p24-encapsulated γ-hPGA NPs strongly induced antigen-specific cellular immunity in mice [35–37]. These results suggest that HIV-1-related antigen-carrying γ-hPGA NPs provide a novel delivery system, and function as an adjuvant for vaccination against HIV-1 infection.

In this study, we evaluated the immune responses in macaques after intranasal and subcutaneous immunization with HIV-1 gp120-carrying γ-hPGA NPs (gp120-NPs). Moreover, to determine whether the vaccination by gp120-NPs can enhance the protective effect against pathogenic viruses, the macaques were intravenously challenged with SHIV-KU-2. Here we report the use of nanoparticles as HIV-1 vaccine adjuvants. Our results demonstrated that gp120-NPs have great potential for the induction of HIV-1 gp120-specific cellular and humoral immunity. However, the macaques immunized with gp120-NPs had an augmented viral load. These results may be helpful for the design of HIV-1 vaccines.

2. Materials and methods

2.1. Nanoparticles (NPs)

γ-PGA (number-average molecular weight, $M_n = 3.8 \times 10^5$) was kindly provided by Meiji Seika Co., Ltd., Tokyo, Japan. The synthetic procedures for the γ-hPGA NPs consisting of γ-PGA conjugated with L-phenylalanine ethylester (γ-PGA-*graft*-Phe) and protein-carrying γ-hPGA NPs have been described previously [35,36]. The mean diameter of the γ-hPGA NPs in aqueous solution was measured by a dynamic light scattering (DLS) method using a Zetasizer Nano ZS (Malvern Instruments, UK). The diameter of the NPs was about 200 nm.

2.2. Preparation of gp120-encapsulated γ-hPGA NPs for intranasal vaccination

Recombinant HIV-1 III_B envelope glycoprotein gp120 (Immuno Diagnostics, Woburn, MA) was chosen for the immunization experiments, and encapsulated into the γ-hPGA NPs (gp120-NPs). To prepare the gp120-encapsulated γ-hPGA NP, γ-PGA-*graft*-Phe (10 mg/ml in DMSO) was added to the same volume (500 μl) of 500 μg/ml recombinant gp120 to yield a translucent solution. The resulting solution was centrifuged at 14,000 × *g* for 15 min, repeatedly rinsed to remove the organic solvents, and prepared to a final particle concentration of 20 mg/ml. The gp120 loading content into the NPs was measured by the Lowry method, as previously described [35]. The amount of encapsulated gp120 into the NPs was 10 μg per mg NP.

2.3. Preparation of gp120-surface immobilized γ-hPGA NPs for subcutaneous vaccination

To prepare the gp120-immobilized γ-hPGA NPs, the carboxyl group of the γ-hPGA NPs (10 mg/ml) was first activated by water-soluble carbodiimide (1 mg/ml) for 20 min. The NPs (5 mg/ml) obtained by centrifugation (14,000 × *g* for 15 min) were suspended in 125 μg/ml gp120, and the mixture was incubated at 4 °C for 24 h. After the reaction, the centrifuged NPs were washed twice with PBS. The resulting solution was prepared to a final particle concentration of 20 mg/ml. The amount of gp120 immobilized onto the NPs was 10 μg per mg NP.

2.4. Animals

Nine rhesus macaques (*Macaca mulatta*) of the Indian origin, which spread in Japan, were used in this study. All macaques were serologically negative for simian immunodeficiency virus (SIV) and simian T cell lymphotropic virus type 1. The macaques were housed in P3 level isolators throughout the experimental period. All experiments were carried out in accordance with regulations approved by the Institutional Animal Care and Use Committee of the Institute for virus Research, Kyoto University.

2.5. Vaccination of macaques

Prior to immunization, the macaques were anesthetized by an intramuscular injection of ketamine chloride. Nine macaques were divided into three groups. Three macaques in the gp120-NP group (MM471, MM472 and MM473) were immunized with gp120-carring γ-hPGA NPs, gp120-alone group (MM471, MM472 and MM473) were immunized with gp120 only, and the 3 macaques in the PBS group (MM474, MM475 and MM476) were immunized with phosphate buffered saline (PBS) as a naive control. Each of three macaques was intranasally immunized at 0, 4, and 8 weeks. At each immunization, 0.5 ml of the inoculum (containing 100 μg of gp120 protein encapsulated into or not into 10 mg of NP) was slowly dripped using a pipette tip into both nasal cavities. In addition, these macaques received subcutaneous injections in close proximity to the axillary lymph nodes at 12 and 16 weeks with 1.5 ml of the inoculum containing 300 μg of gp120 immobilized onto or not onto 30 mg of NP.

2.6. Challenge inoculation to macaques

SHIV KU-2 was used in the experiments. SHIV KU-2 is a polyclonal chimeric SHIV generated by in vivo passage of SHIV-4, containing the envelope gene of HIV-1 HXBc2 [38]. The SHIV-KU-2 virus stock for the challenge experiments was produced by culture in rhesus macaque peripheral blood mononuclear cells (PBMCs), and stored in liquid nitrogen until use. The 50% tissue culture infectious dose ($TCID_{50}$) of the virus stock was determined by culture in M8166 cells. At 4 weeks after the last immunization, all nine macaques were intravenously challenged with SHIV-KU-2. For the intravenous challenge, macaques were anesthetized, and then 1×10^5 $TCID_{50}$ of the virus inoculum was used. Blood samples were periodically collected from all macaques. The PBMCs were separated from ACD-A blood by Percoll density centrifugation.

2.7. Quantitative analysis of anti-HIV-1 gp120 IgG and IgA antibodies

HIV-1 gp120-specific IgG and IgA antibody levels in the plasma were measured by an ELISA method. A 96-well microplate (Nunc-Immuno™ Modules, Maxisorp™, Nalga-Nunc, Rochester, NY) was coated with recombinant HIV-1 III_B gp120 (Immuno Diagnostics) at a concentration of 1 μg/ml in 0.1 M Na_2CO_3–$NaHCO_3$ buffer (pH 9.6). The plate was left over night at 4 °C, washed with washing buffer (containing 0.15 M NaCl and 0.05% Tween 20), and treated with a blocking buffer (1% BSA, 1% skim milk in washing buffer) for 2 h at room temperature. To measure the IgG and IgA antibodies, the plasma was 100-fold diluted with blocking buffer, and applied to the plate. The plate was the incubated overnight at 4 °C. After washing with washing buffer, peroxidase-conjugated goat anti-monkey IgG or IgA (Kirkegaard & Perry Laboratories, Gaithersburg, MD) was added to the plate and incubated for 2 h at room temperature. The plate was then washed, and treated with *O*-phenylenediamine dehydrochloride (OPD, Wako Pure Chemical, Osaka, Japan) for 5 min and stopped with 2N H_2SO_4. The specific absorbances were read at 490/690 nm with a microplate reader. The titers of anti-HIV1/2 antibodies in the plasma of all macaques after challenge with SHIV-KU-2 were measured by the particle agglutination (PA) method (Genedia HIV-1/2 mix PA kit, Fujirebio Inc., Tokyo, Japan) following the manufacturer's recommendations.

2.8. Antigen specific proliferation assay

PBMCs from the vaccinated macaques were cultured in triplicate in a 96-well plate (2×10^5 cells/well) with 200 μl of RPMI 1640 medium in the presence of 0.5 μg recombinant HIV-1 III_B gp120 (Immuno Diagnostics) or 1 μg SIV_{mac251} p27 purified native protein (Advanced Biotechnologies, Inc., Columbia, MD) for 72 h. Next, the antigen specific proliferations were measured by BrdU incorporation into the stimulated PBMCs using a cell proliferation ELISA kit (Roche Diagnostic CmbH, Mannheim, Germany) following the manufacturer's recommendations. The stimulation index (SI) for cell activity was calculated using the following formula: stimulation index (SI) = (OD stimulated – blank)/(OD non-stimulated – blank). A SI value above 2.5 was considered as 'antigen-specific' stimulation. Concanavalin A (Con A) was used as a polyclonal stimulator positive control.

2.9. IFN-γ ELISPOT assay

An enzyme-linked immunospot (ELISPOT) assay was performed by stimulating unfractionated PBMCs with recombinant HIV-1 III_B gp120 (Immuno Diagnostics) or SIV_{mac251} p27 purified native protein (Advanced Biotechnologies). MultiScreen 96-Well Plates (Millipore Corporation, Bedford, MA) were coated overnight (100 μl/well) at 37 °C with diluted monoclonal antibody GZ-4 (MABTECH Inc., Mariemont, OH). The plates were then washed 3 times with PBS (–) containing 0.25% Tween 20 (PBS/0.25% Tween 20). The PBMCs were plated in triplicate at 5×10^5/well in 200 μl with either medium alone, 0.5 μg HIV-1 gp120 or 1 μg SIV_{mac251} p27. Following a 72 h incubation at 37 °C, the plates were washed 3 times with PBS/0.25% Tween 20 and incubated for 4 h at 37 °C with a 1:1000 dilution of biotinylated monoclonal antibody 7-B6-1 (MABTECH Inc). Following 3 washes with PBS/0.25% Tween 20, the plates were incubated for 2 h at room temperature with a 1:1000 dilution of streptavidin-alkaline phosphatase (MABTECH Inc). The plate was developed with a BCIP:NBT:0.1 M Tris buffer solution (1:1:10) mixture (Kirkegaard & Perry Laboratories, Gaithersburg, Maryland). Thereafter, the plate was washed 3 times with PBS/0.25% Tween 20, and the reaction stopped by tap water, the plate air dried, and the spots were then read. The mean number of spots from triplicate wells was then calculated for each animal. The data were expressed as the mean number of spots per 10^6 PBMC.

2.10. Quantification of plasma viral RNA loads

Virion-associated SHIV RNA loads in the plasma were measured by real-time reverse transcription (RT)-PCR assay [39]. Briefly, total RNA was prepared from the plasma (140 μl) of each macaque with a QIAamp Viral RNA kit (QIAGEN, Hilden, Germany). RT reactions and PCR were performed by a Platinum qRT-PCR ThermoScript One-Step System (Invitrogen, Carlsbad, CA) using the following primers for the gag region: SIV2-696F (5′-GGA AAT TAC CCA GTA CAA CAA ATAGG-3′), and SIV2-784R (5′-TCT ATC AAT TTT ACC CAGGCA TTT A-3′). A labeled probe, SIV2-731T (5′-Fam-TGTCCA CCT GCC ATT AAG CCC G-Tamra-3′), was used for the detection of the PCR products. These reactions were performed with a Prism 7700 Sequence Detector (Applied Biosystems, Foster City, CA) and analyzed using the manufacturer's software. For each run, a standard curve was generated from dilutions whose copy numbers were known, and the RNA in the plasma samples was quantified based on the standard curve. Under these conditions, the detection limit was 1000 copies/ml.

2.11. Flow cytometric analysis

The frequency of $CD4^+$ T lymphocytes in the whole blood was examined by flow cytometry. Blood samples were immunostained with anti-CD3 (FN-18-FITC; Bio Source, Camarillo, CA), anti-CD4 (L200-APC; Becton-Dickinson, Franklin Lakes, NJ), anti-CD8 (SK1-PerCP; Becton-Dickinson), anti-CD28 (CD28.2-PE;

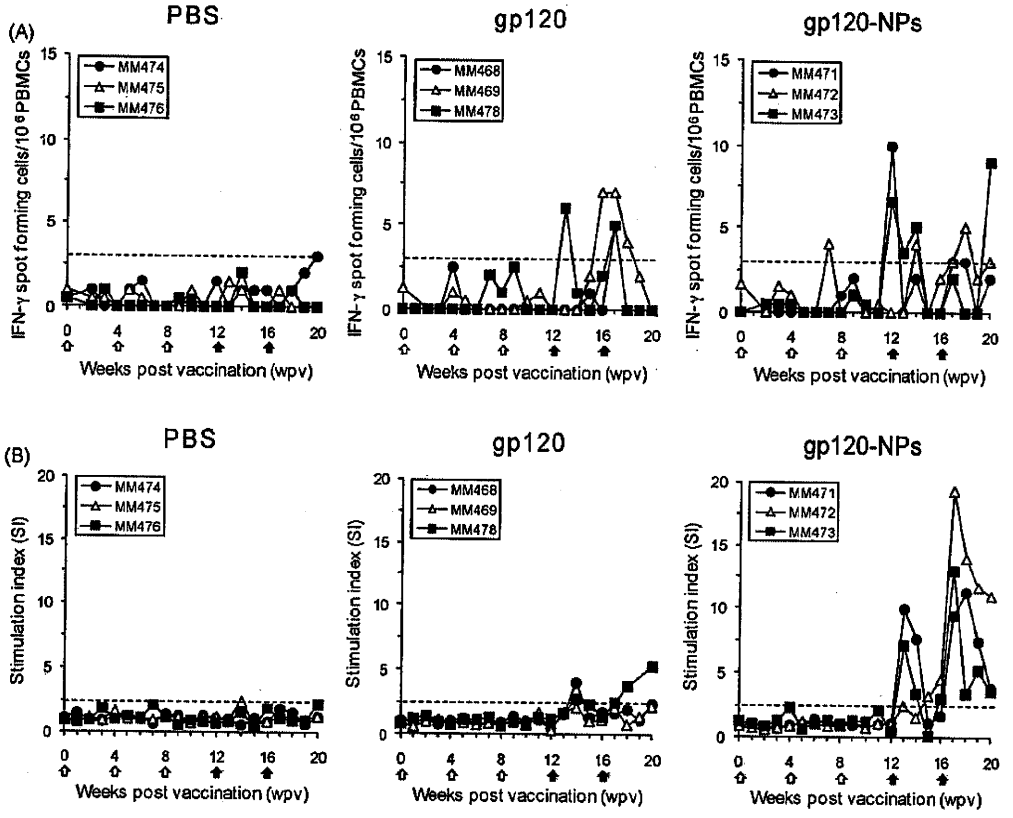

Fig. 1. gp120-specific (A) IFN-γ ELISPOT responses and (B) proliferation responses in PBMCs from macaques immunized with gp120-NPs, gp120-alone and PBS control. The PBMCs from immunized macaques were collected at an interval of 1-week. The results of three individual macaques per group are shown. The white arrows indicate the times of intranasal immunization, and the black arrows indicate the times of subcutaneous immunization. (A) The number of IFN-γ secreting PBMCs detected by ELISPOT after stimulation with gp120. The data represent the mean number of spots per million cells detected in duplicate cultures, after subtracting the mean number of spots found in duplicate control cultures of PBMCs in medium alone. (B) The proliferation of the PBMCs was measured by Brd-U uptake after stimulation with gp120, and is expressed as the stimulation index (SI), as described in Section 2. The cut off value was 2.5 for the SI.

Coulter-Immunotec) and anti-CD95 (DX2-FITC; Becton-Dickinson) antibodies. After hemolysis of the whole blood using FACS™ Lysing Solution (BD PhorMingen, San Diego, CA), each labeled lymphocyte was analyzed on a FACScalibur™ (Becton-Dickinson). The blood was assayed with an automated blood cell counter (F-820; Sysmex, Kobe, Japan).

3. Results

3.1. Vaccination of macaques with gp120-NPs

It is known that gp120-NPs induced efficient cellular immune responses after only one single intranasal immunization in mice [36]. At the beginning, we expected that the gp120-NPs would induce an immune response by very few vaccinations. Nine macaques were intranasally immunized with gp120-NPs (MM471, MM472 and MM473: gp120-NP group), gp120-alone (MM468, MM469 and MM478: gp120-alone group) or PBS as naive controls (MM474, MM475 and MM476: PBS group). However, all macaques had to be subcutaneously immunized twice with additional vaccinations, because their immune responses were insufficient after 3 intranasal immunizations.

To examine whether HIV-1 gp120-specific cellular immunity was induced in the vaccinated macaques, the number of gp120-specific spot forming cells (SFCs) secreting IFN-γ of PBMCs in each macaque group were measured by an ELISPOT assay (Fig. 1A). In all macaques from the PBS group, less than 3 gp120-specific SFC spots were detected throughout the measurement period. On the other hand, in all macaques from the gp120-alone and gp120-NP groups, more than 5 spots of gp120-specific SFCs were detected. The increase of gp120-specific SFCs in the gp120-NP group was earlier than in the gp120-alone group.

Next, we measured the antigen specific proliferation activities by determining the ratio of Brd-U incorporated by PBMCs in the presence of HIV-1 gp120 (Fig. 1B). In the PBS group, gp120-specific proliferation activities were not detected during the measurement period (stimulation index: SI < 2.5). Furthermore, in the gp120-alone and gp120-NP groups, no significant proliferative responses were detected throughout the intranasal immunization period. But after subcutaneous immunization in the gp120-alone and gp120-NP groups, an increase in the activities (SI > 2.5) was detected. Higher proliferative responses were observed in all macaques from the gp120-NP group than in the gp120-alone group.

To examine whether gp120-specific humoral immunities were induced in the vaccinated macaques, we measured anti-gp120-specific antibody levels in the plasma with the ELISA method (Fig. 2). Although, plasma anti-gp120-specific IgG and IgA antibodies were non-specifically detected at higher levels in one macaque from the PBS group (MM476), no significant increase in titer was observed in PBS group throughout the measurement period. Furthermore, in the gp120-alone and gp120-NP groups, no significant increase in titer was detected throughout the intranasal immunization period except for the plasma anti-gp120 IgG antibodies from one macaque (MM469) in the gp120-alone group. After subcutaneous immunization, in all macaques from the gp120-alone and gp120-NP groups, both plasma anti-gp120 IgG and IgA antibodies

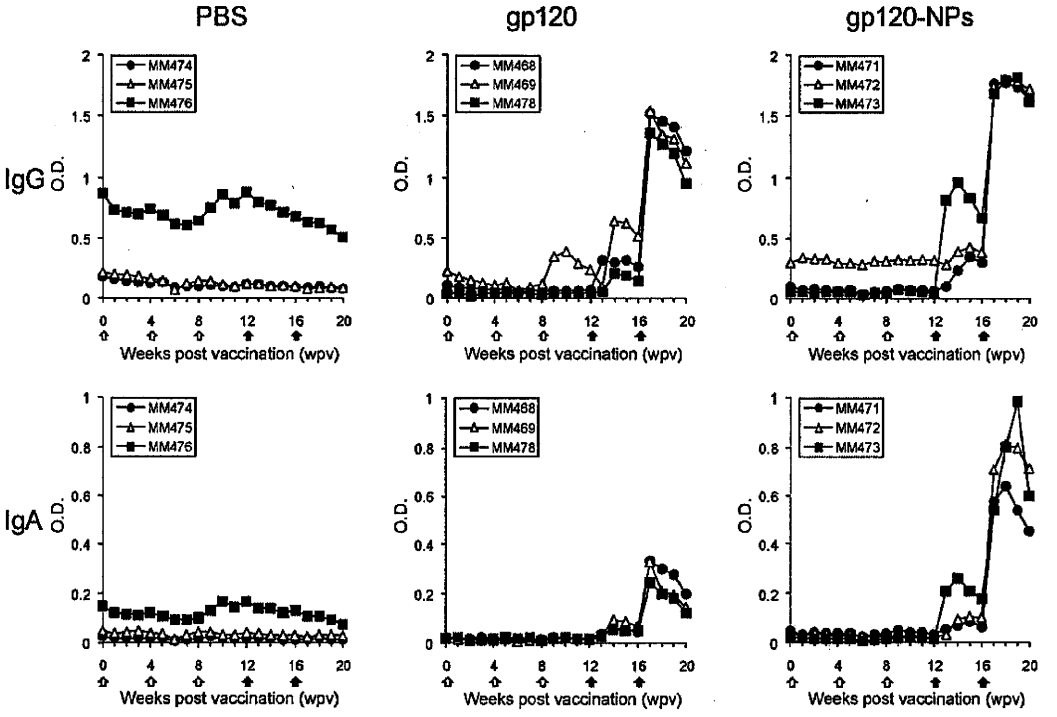

Fig. 2. Anti-HIV-1 gp120 IgG and IgA antibody levels in the plasma of macaques immunized with gp120-NPs, gp120-alone and PBS control. Plasma samples were collected at an interval of 1-week. The levels of gp120-specific IgG and IgA antibodies were measured by ELISA. Plasma samples were assayed after 100-fold dilution. The data are expressed as the optical density (O.D.). The white arrows indicate the times of intranasal immunization, and the black arrows indicate the times of subcutaneous immunization.

were clearly increased. A higher titer was detected in all macaques from the gp120-NP group than in the gp120-alone group. Thus, additional subcutaneous immunizations of 300 μg of gp120 antigen induced clear immune responses in the macaques, although the first 3 bouts of intranasal immunizations with 100 μg of gp120 antigen were insufficient. The induced cellular and humoral immune responses were higher in the gp120-NP group than in the gp120-alone group.

3.2. Intravenous challenge of the vaccinated macaques with SHIV-KU-2

To evaluate the protective effects provided by immunization with gp120-NP, a pathogenic virus, SHIV-KU-2, was intravenously challenged to vaccinated macaques 4 weeks after the last immunization. The plasma viral RNA load and $CD4^+$ T cell counts in the peripheral blood were then monitored.

The plasma viral RNA load in two macaques from the PBS group (MM474 and 475) increased with a peak of 10^6–10^7 copies/ml at 1-week post challenge (wpc), and one macaque (MM476) showed over 10^8 copies/ml after 2 wpc. Then, the viral load in all macaques decreased to below the 10^4 copies/ml after 10 wpc (Fig. 3). On the other hand, in all macaques from the gp120-alone and gp120-NP groups, the viral RNA load peaked at over 10^8 copies/ml at 2 wpc. Furthermore, two of the three macaques in the gp120-NP group (MM472 and 473) showed over 10^6 copies/ml after 10 wpc, although the viral RNA load of the other macaques decreased to below 10^5 copies/ml at those time points. Thus, the challenged virus had replicated more in the vaccinated groups than in the PBS control group. Furthermore, this tendency was more intense in the gp120-NP group than in the gp120-alone group.

The number of $CD4^+$ T cells in the peripheral blood of all macaques in the gp120-alone and gp120-NP groups decreased drastically to below 20% of the pre-challenge levels by 3 wpc, although the $CD4^+$ T cells were not so severely decreased in two of the three macaques in the PBS control group (MM474 and 475) (Fig. 4A). Thereafter, in two macaques from the gp120-NP group (MM472 and MM473) and one macaque from the gp120-alone group (MM469) remained below 20% of the pre-challenge levels until 12 wpc, according to the results of the plasma viral RNA load. Thus, the $CD4^+$ T cells in the peripheral blood were more severely decreased in the vaccinated groups than in the PBS control group. Furthermore, this tendency was more pronounce in the gp120-NP group than in the gp120-alone group.

To understand the decrease in the $CD4^+$ T cell population in the peripheral blood in more detail, we analyzed the $CD4^+$ T cell subpopulations using a CD95 marker. In two of the three macaques from the PBS group (MM474 and MM475), the $CD95^-$ naive $CD4^+$ T cell subpopulation remained over 30% after challenge (Fig. 4B). On the other hand, in all macaques from the gp120-alone and gp120-NP groups and one macaque from the PBS group (MM476), the naive $CD4^+$ T cell subpopulation decreased to below 20%. In all macaques, the $CD95^+$ memory $CD4^+$ T cell subpopulation transiently increased at 1 wpc and thereafter, in most of the macaques, it was maintained at the pre-challenge levels (20–40%) except for two macaques from the gp120-NP group (MM472 and MM473). The memory $CD4^+$ T cell population of these macaques decreased to below 10% after 3 wpc, and did not recover until 12 wpc (data not shown). Thus, in those macaques who showed a high viral load and severe $CD4^+$ T cell depletion, the memory $CD4^+$ T cell subpopulation was more severely injured as compared to the other macaques.

3.3. Virus-specific immune responses after the challenge infection of SHIV-KU-2

To assess the systemic immune responses in vaccinated macaques after the intravenous challenge infection, the virus-specific antibody levels in the plasma of macaques challenged

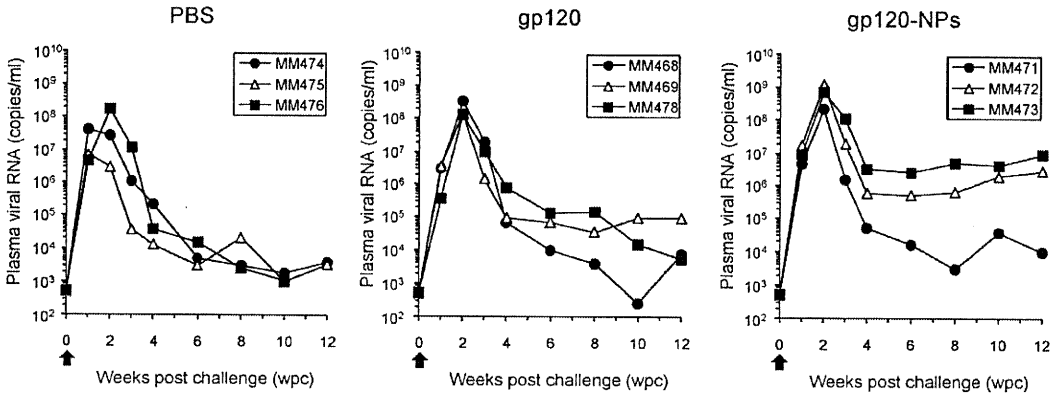

Fig. 3. Plasma viral RNA loads in the peripheral blood of SHIV-KU-2 infected macaques after intravenous inoculation with SHIV-KU-2. The unimmunized (PBS) and immunized (gp120-alone and gp120-NPs) macaques were intravenously challenged with SHIV-KU-2. The plasma viral RNA loads were measured by RT-PCR with a detection limit of 5×10^2 copies/ml. The black arrows indicate the time of challenge with SHIV-KU-2.

with SHIV-KU-2 were measured by the particle agglutination test (Table 1). In the gp120-alone and gp120-NP groups, the initial antibody responses were delayed as compared to the PBS group. In particular, MM472 and MM473 of the gp120-NP group had high viral loads, and the antibody titers were also low in these macaques. These results suggest that there was no protective effect against SHIV-KU-2 in both gp120-NP and gp120-alone groups, in contrast to the immunization-increased viral proliferation.

To assess the effects of the immunization, the lymphocyte proliferation activities after SHIV-KU-2challenge were measured by determining the ratio of Brd-U incorporated by PBMCs in the presence of HIV-1 gp120 and SIV p27 (Fig. 5). First, the gp120-specific lymphocyte proliferation activities were increased in two macaques from the PBS group at 2, 4 (MM476) and 8 wpc (MM475). In two macaques from the gp120-alone group (MM468 and MM469), an increase in proliferative activities could be detected at 2 and 3 wpc. On the other hand, in three macaques from the gp120-NP group, an increase in proliferative responses was observed after 1 wpc (MM472 and MM473) and 2 wpc (MM471). In other words, the increase in activity in the gp120-NP group could be detected earlier than any other group. p27-specific lymphocyte proliferation activities were increased in three macaques from the PBS group at 2 wpc (MM475 and MM476) and 3 wpc (MM474). After 4 wpc in the PBS group, higher proliferative responses were observed in

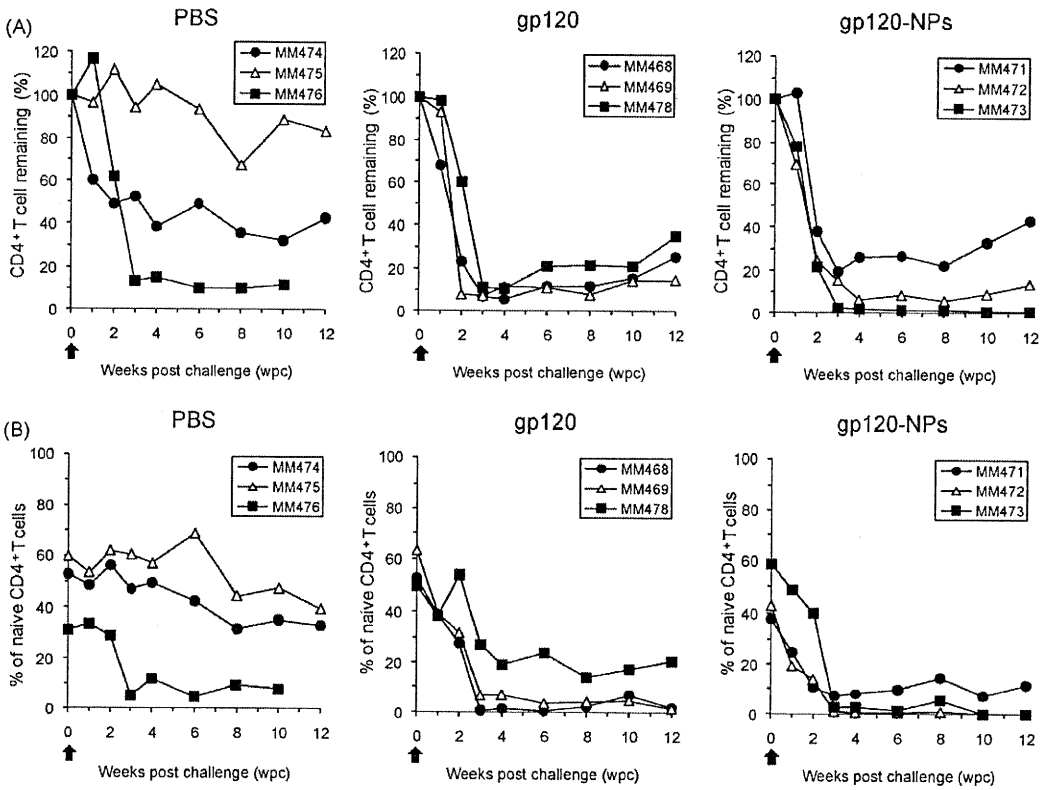

Fig. 4. The number of (A) $CD4^+$ T cells and (B) $CD95^-$ naive $CD4^+$ T cells in the peripheral blood of SHIV-KU-2 infected macaques after an intravenous inoculation with SHIV-KU-2. (A) The number of $CD4^+$ T cells was determined by flow cytometry. The data are expressed as a percent of the cell counts immediately before challenge. (B) Sequential changes in the proportion of the subpopulation (CD95 negative naive cells) of the peripheral blood $CD4^+$ T cells. The percentage of these cells in the $CD4^+$ T cells was determined by flow cytometry. The black arrows indicate the time of challenge with SHIV-KU-2.

Table 1
HIV-1/2 specific antibody responses in the plasma obtained from vaccinated macaques after the intravenous SHIV-KU-2 challenge.

Groups	Macaques	Weeks post challenge (wpc)							
		1	2	3	4	6	8	10	12
PBS	MM474	n.d.	4096	>16,384	>16,384	>16,384	>16,384	>16,384	>16,384
	MM475	n.d.	4096	>16,384	>16,384	>16,384	>16,384	>16,384	>16,384
	MM476	n.d.	8192	>16,384	>16,384	>16,384	>16,384	>16,384	-
gp120	MM468	n.d.	1024	1024	4096	>16,384	>16,384	>16,384	>16,384
	MM469	n.d.	4096	>16,384	>16,384	>16,384	>16,384	>16,384	>16,384
	MM478	n.d.	256	512	8192	>16,384	>16,384	>16,384	>16,384
gp120-NPs	MM471	n.d.	4096	>16,384	>16,384	>16,384	>16,384	>16,384	>16,384
	MM472	32	4096	4096	2048	>16,384	8192	4096	2048
	MM473	n.d.	1024	1024	256	512	512	256	128

Antibodies to HIV *gag* p24 and *env* gp41 in the plasma were measured by the PA method. The data indicated as the titer of serial dilution. n.d.: not detected.

all macaques. In all macaques from the gp120-alone group, the increase in activity could be detected after 2 wpc. On the other hand, in only one macaque from the gp120-NP group (MM471) with a low viral load, an increase in activity was observed after 3 wpc. In the gp120-NP and gp120-alone groups, an increased plasma viral RNA load, and a reduction in $CD4^+$ T cells in the peripheral blood, and gp120-specific lymphocyte proliferation were identified at 1–3 wpc. However, in the PBS group, p27-specific lymphocyte proliferation was identified at the same time, and was higher than in the immunized group after 4 wpc. These results suggest that immunization with gp120-NPs or gp120-alone enhanced gp120-specific immunity, but immunity to the gp120 antigen did not become effective against viral infection or viral proliferation.

4. Discussion

Polymeric nanoparticles have been investigated as an efficient delivery system to APCs for a protein antigen [40]. Therefore biodegradable NPs consisting of γ-PGA derived from *Bacillus* represent a system with efficient immune induction [41–48] and safety [45,46], since it is specifically taken up by dedicated APCs such as DCs [34,44], and is easily disintegrated by proteases [49]. In immune induction experiments using mice with HIV-1 *env*-gp120 carrying γ-hPGA NPs (gp120-NPs), it was shown that both cellular and humoral immune responses were efficiently induced by a low number of vaccinations, suggesting the possibility of use as an efficient vaccine candidate for HIV-1 infection [36]. However, it is unknown whether the immune responses induced in the mouse have protective effects against HIV infection, because HIV-1 is not contagious to mice. Therefore, we immunized rhesus macaques with gp120-NPs in this study to clarify the immune induction capabilities of gp120-NPs and their protective effects against viral infection using a SHIV infection system, because this could not be confirmed with the mouse model.

In the mouse experiments, potent specific cellular immunity was induced with a single intranasal administration of gp120-NPs

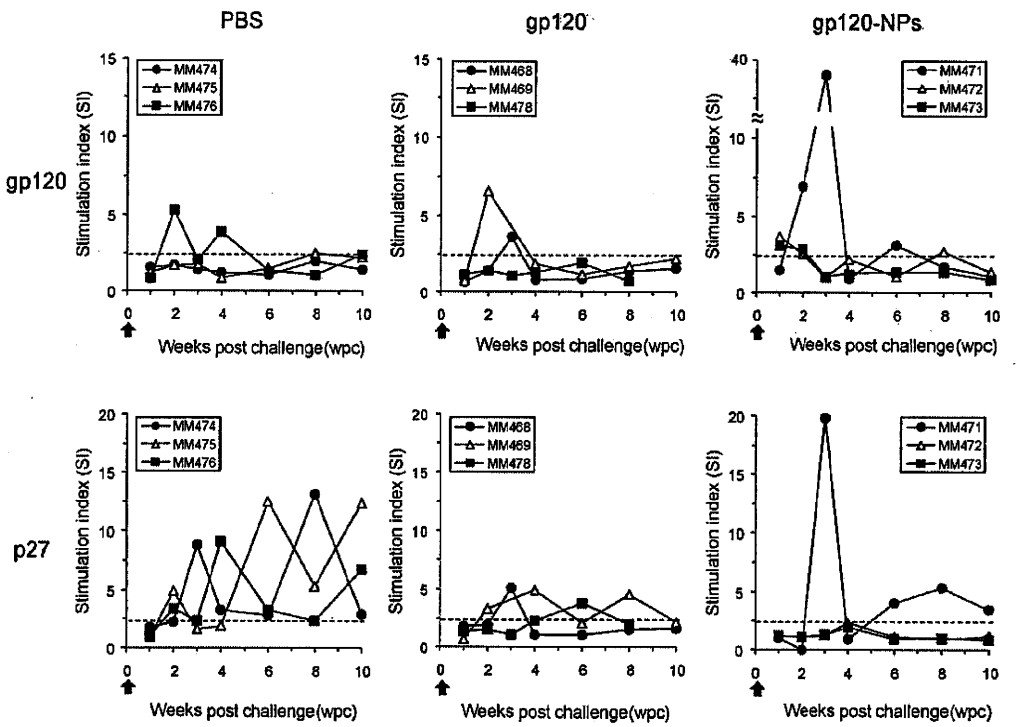

Fig. 5. Antigen-specific lymphocyte proliferation responses in PBMCs from macaques challenged with SHIV-KU-2. The proliferation of the PBMCs was measured by Brd-U uptake after stimulation with gp120 or p27, and was expressed as a stimulation index (SI) as described in Section 2. The cut off value is 2.5 for the SI. The arrows indicate the time of challenge with SHIV-KU-2.

[36]. It has also been reported that mucosal immunization with an HIV-1 vaccine can induce mucosal and systemic HIV-1-specific humoral and cellular immune responses in macaques [20,50,51]. Therefore, we selected intranasal immunization as the administration route of vaccines. However, we determined that three intranasal administrations with 100 μg of gp120-NPs were not able to induce a sufficient immune response in the macaques. Therefore, we performed two additional subcutaneous administrations with 300 μg of gp120-NPs. In this experiment, 100 μg of gp120 was used for each nasal administration. This quantity was decided by a calculation from the optimal amount per weight obtained from mouse experiments. Other research groups administered it intramuscularly or subcutaneously, with more amount of gp120, and obtained antigen-specific cellular immunity and antibody responses [52,53], although they used a different antigen delivery system. In our particulate delivery system, a greater amount of antigen was necessary to induce a specific immune response in macaques than in mice. An additional two subcutaneous administrations with 300 μg of gp120-NPs induced not only cellular immune responses, but also humoral antibody responses (IgG and IgA), which was poorly induced in the mouse experiments [35], indicating a boost effect in macaques. After the subcutaneous immunization, the increase in gp120-specific IFN-γ producing cells, the increase in gp120-specific cell proliferation activity and the anti-gp120 antibody titer (IgG and IgA) in the plasma were confirmed in all macaques immunized with gp120-NPs and gp120-alone. In both cellular and humoral immune responses, the degree of immune induction was clearly stronger in the gp120-NP immunized macaques than in the gp120-alone immunized macaques. Thus, it became clear that γ-hPGA NPs had an immune reinforcement effect not only in the mice, but also in the rhesus macaques. However, the numbers of gp120-specific SFCs in the gp120-NP group obtained from ELISPT assay were low at less than 10 spots per million PBMCs. These results suggest that antigen-specific CD8 T cell responses were not or poorly induced by the vaccination of gp120-NPs. Consequently, CD4 T cell responses were primarily enhanced in macaques immunized with gp120-NPs.

To examine the protective effects of the gp120-specific immune responses induced by gp120-NPs against viral infection, a challenge inoculation with pathogenic SHIV-KU2 was performed in immunized macaques. Against our expectations, no protective effect was observed. Instead, a promotion of viral growth was observed in immunized macaques as compared to naive control macaques. Furthermore, the degree of reinforcement of the infection was stronger in the gp120-NP immunized macaques than in the gp120-alone immunized macaques. The gp120-specific immune responses induced by vaccination correlated with the promotion of viral growth in between groups. However, there was no definite the correlation between the immune responses and viral road of within-group. Since the target cells for primate lentivirus infection are immune cells such as $CD4^+$ T cells and macrophages, the only useful immune reaction should be activated protection against viral infection. In other words, there is a case for promoting viral replication by inappropriate or insufficient immune responses. For example, there were some antibodies reinforcing the HIV-1 infection [54,55], and HIV-1 is preferentially contagious to memory $CD4^+$ T cells, which are specific for HIV-1 antigens [56]. In this study, we used gp120 as the antigen based on the result that the immune response against *env* was better than that against *gag* in a mouse study [36,37]. The number of $CD4^+$ T cells in the peripheral blood decreased conspicuously at the same time as the immune response specific for gp120 appeared early after virus inoculation in the gp120-NP and gp120-alone vaccinated groups. On the other hand, in the naive control group, the immune response specific for p27 (*gag*) was detected, but not the immune response specific for gp120 (*env*) early after the virus inoculation. Thus, the $CD4^+$ T cells in the peripheral blood were maintained without any decrease in 2 out of 3 naive control macaques. Recently, it has been reported that the strength of the specific immune response against *gag*, i.e. the internal protein structure of the virus is correlated to the decrease in the quantity of virus in the peripheral blood of HIV-1 infected patients. In contrast, the strength of the specific immune responses against the *env* in the crust protein and accessory proteins are correlated to the increase in the quantity of blood virus [57]. Our result that the vaccination of rhesus macaques inducing a specific immune response against *env*-gp120 showed an enhancement of viral replication was consistent with the observations in HIV-1 infected patients, supporting the importance of antigen selection for HIV-1 vaccine development. Moreover, some groups have recently argued that activated $CD4^+$ T cells induced by vaccination in macaques can be an attractive target for SIV infection [58,59]. It is likely that the macaques immunized with gp120-NPs were primarily enhanced gp120-specific CD4 T cell responses but not CD8 T cell. The balance of CD4 and CD8 T cell mediated responses induced by vaccination may be critical in determining viral exclusion and replication.

The total picture of the immune system which is truly important for infection control in individuals infected with the AIDS virus is not yet clarified, and the further accumulation of basic information about the immune correlates for protective immunity is necessary. In our previous project, the partial protective effects of viral replication was obtained in vaccinated macaques by using different nanoparticles connecting the inactivated whole virus particles, not a refined protein [28]. The whole virion is considered to include many kinds of antigens acting for infection restraint and/or promotion. It may be possible to induce only effective immune responses acting for infection restraint with a biodegradable nanoparticle vaccine, distinguishing the restraint-related and promotion-related antigens by a detailed examination of the antigen enclosed in the γ-hPGA NPs in the future. Although cell-mediated immunity against peptide epitopes of viral structural proteins is the mainstream for vaccine development research, other poorly analyzed target antigens such as glycolipids, lipoproteins and nuclear antigens may also have to be examined.

In this study, it was demonstrated that biodegradable nanoparticles composed of amphiphilic γ-PGA have a reinforcement effect for immune responses, and have an impact on important immune cell populations participating in viral replication in infected individuals, although the result was the opposite to our expectation. It is important to ascertain the correct antigen stimulation to guide the patient's immunity to act on infection defense and viral replication restraint effectively using a primate experimental infection model. These biodegradable nanoparticles are expected to be useful as an antigen delivery tool in AIDS vaccine development research.

Acknowledgment

This work was supported by CREST from the Japan Science and Technology Agency (JST).

References

[1] Letvin NL. Correlates of immune protection and the development of a human immunodeficiency virus vaccine. Immunity 2007;27:366–9.
[2] Pomerantz RJ, Horn DL. Twenty years of therapy for HIV-1 infection. Nat Med 2003;9:867–73.
[3] Chun TW, Fauci AS. Latent reservoirs of HIV: obstacles to the eradication of virus. Proc Natl Acad Sci USA 1999;96:10958–61.
[4] Zhao Z, Leong KW. Controlled delivery of antigens and adjuvants in vaccine development. J Pharm Sci 1996;85:1261–70.
[5] Singh M, O'Hagan D. Advances in vaccine adjuvants. Nat Biotechnol 1999;17:1075–81.
[6] Storni T, Kundig TM, Senti G, Johansen P. Immunity in response to particulate antigen-delivery systems. Adv Drug Deliv Rev 2005;57:333–55.
[7] Greenland JR, Letvin NL. Chemical adjuvants for plasmid DNA vaccines. Vaccine 2007;25:3731–41.

[8] O'Hagan DT, Lavelle E. Novel adjuvants and delivery systems for HIV vaccines. AIDS 2002;16:115–24.
[9] Reddy ST, Swartz MA, Hubbell JA. Targeting dendritic cells with biomaterials: developing the next generation of vaccines. Trends Immunol 2006;27:573–9.
[10] Waeckerle-Men Y, Groettrup M. PLGA microspheres for improved antigen delivery to dendritic cells as cellular vaccines. Adv Drug Deliv Rev 2005;57:475–82.
[11] Shibata R, Igarashi T, Haigwood N, Buckler-White A, Ogert R, Ross W, et al. Neutralizing antibody directed against the HIV-1 envelope glycoprotein can completely block HIV-1/SIV chimeric virus infections of macaque monkeys. Nat Med 1999;5:204–10.
[12] Mascola JR, Stiegler G, VanCott TC, Katinger H, Carpenter CB, Hanson CE, et al. Protection of macaques against vaginal transmission of a pathogenic HIV-1/SIV chimeric virus by passive infusion of neutralizing antibodies. Nat Med 2000;6:207–10.
[13] Parren PW, Marx PA, Hessell AJ, Luckay A, Harouse J, Cheng-Mayer C, et al. Antibody protects macaques against vaginal challenge with a pathogenic R5 simian/human immunodeficiency virus at serum levels giving complete neutralization in vitro. J Virol 2001;75:8340–7.
[14] Borrow P, Lewicki H, Hahn BH, Shaw GM, Oldstone MB. Virus-specific CD8+ cytotoxic T-lymphocyte activity associated with control of viremia in primary human immunodeficiency virus type 1 infection. J Virol 1994;68:6103–10.
[15] Ogg GS, Jin X, Bonhoeffer S, Dunbar PR, Nowak MA, Monard S, et al. Quantitation of HIV-1-specific cytotoxic T lymphocytes and plasma load of viral RNA. Science 1998;279:2103–6.
[16] Matano T, Shibata R, Siemon C, Connors M, Lane HC, Martin MA. Administration of an anti-CD8 monoclonal antibody interferes with the clearance of chimeric simian/human immunodeficiency virus during primary infections of rhesus macaques. J Virol 1998;72:164–9.
[17] Schmitz JE, Kuroda MJ, Santra S, Sasseville VG, Simon MA, Lifton MA, et al. Control of viremia in simian immunodeficiency virus infection by CD8+ lymphocytes. Science 1999;283:857–60.
[18] McMichael AJ, Hanke T. HIV vaccines 1983–2003. Nat Med 2003;9:874–80.
[19] Verschoor EJ, Mooij P, Oostermeijer H, van der Kolk M, ten Haaft P, Verstrepen B, et al. Comparison of immunity generated by nucleic acid-MF59-, and ISCOM-formulated human immunodeficiency virus type 1 vaccines in Rhesus macaques: evidence for viral clearance. J Virol 1999;73:3292–300.
[20] Yoshino N, Lu FX, Fujihashi K, Hagiwara Y, Kataoka K, Lu D, et al. A novel adjuvant for mucosal immunity to HIV-1 gp120 in nonhuman primates. J Immunol 2004;173:6850–7.
[21] Koopman G, Bogers WM, van Gils M, Koornstra W, Barnett S, Morein B, et al. Comparison of intranasal with targeted lymph node immunization using PR8-Flu ISCOM adjuvanted HIV antigens in macaques. J Med Virol 2007;79:474–82.
[22] Barnett SW, Srivastava IK, Kan E, Zhou F, Goodsell A, Cristillo AD, et al. Protection of macaques against vaginal SHIV challenge by systemic or mucosal and systemic vaccinations with HIV-envelope. AIDS 2008;22:339–48.
[23] Flynn NM, Forthal DN, Harro CD, Judson FN, Mayer KH, Para MF, et al. Placebo-controlled phase 3 trial of a recombinant glycoprotein 120 vaccine to prevent HIV-1 infection. J Infect Dis 2005;191:654–65.
[24] Bogers WM, Cheng-Mayer C, Montelaro RC. Developments in preclinical AIDS vaccine efficacy models. AIDS 2000;14:141–51.
[25] Akagi T, Kawamura M, Ueno M, Hiraishi K, Adachi M, Serizawa T, et al. Mucosal immunization with inactivated HIV-1-capturing nanospheres induces a significant HIV-1-specific vaginal antibody response in mice. J Med Virol 2003;69:163–72.
[26] Akagi T, Ueno M, Hiraishi K, Baba M, Akashi M. AIDS vaccine: intranasal immunization using inactivated HIV-1-capturing core-corona type polymeric nanospheres. J Control Release 2005;109:49–61.
[27] Wang X, Akagi T, Akashi M, Baba M. Development of core-corona type polymeric nanoparticles as an anti-HIV-1 vaccine. Mini-Rev Org Chem 2007;4:281–90.
[28] Miyake A, Akagi T, Enose Y, Ueno M, Kawamura M, Horiuchi R, et al. Induction of HIV-specific antibody response and protection against vaginal SHIV transmission by intranasal immunization with inactivated SHIV-capturing nanospheres in macaques. J Med Virol 2004;73:368–77.
[29] Akagi T, Baba M, Akashi M. Preparation of nanoparticles by the self-organization of polymers consisting of hydrophobic and hydrophilic segments: potential applications. Polymer 2007;48:6729–47.
[30] Matsusaki M, Hiwatari K, Higashi M, Kaneko T, Akashi M. Stably-dispersed and surface-functional bionanoparticles prepared by self-assembling amphipathic polymers of hydrophilic poly(γ-glutamic acid) bearing hydrophobic amino acids. Chem Lett 2004;33:398–9.
[31] Akagi T, Kaneko T, Kida T, Akashi M. Preparation and characterization of biodegradable nanoparticles based on poly(γ-glutamic acid) with L-phenylalanine as a protein carrier. J Control Release 2005;108:226–36.
[32] Akagi T, Kaneko T, Kida T, Akashi M. Multifunctional conjugation of proteins on/into core-shell type nanoparticles prepared by amphiphilic poly(γ-glutamic acid). J Biomater Sci Polym Ed 2006;17:875–92.
[33] Kim H, Akagi T, Akashi M. Preparation of size tunable amphiphilic poly(amino acid) nanoparticles. Macromol Biosci 2009;9:842–8.
[34] Uto T, Wang X, Sato K, Haraguchi M, Akagi T, Akashi M, et al. Targeting of antigen to dendritic cells with poly(γ-glutamic acid) nanoparticles induces antigen-specific humoral and cellular immunity. J Immunol 2007;178:2979–86.
[35] Akagi T, Wang X, Uto T, Baba M, Akashi M. Protein direct delivery to dendritic cells using nanoparticles based on amphiphilic poly(amino acid) derivatives. Biomaterials 2007;28:3427–36.
[36] Wang X, Uto T, Akagi T, Akashi M, Baba M. Induction of potent CD8+ T-cell responses by novel biodegradable nanoparticles carrying human immunodeficiency virus type 1 gp120. J Virol 2007;81:10009–16.
[37] Wang X, Uto T, Akagi T, Akashi M, Baba M. Poly(γ-glutamic acid) nanoparticles as an efficient antigen delivery and adjuvant system: potential for an AIDS vaccine. J Med Virol 2008;80:11–9.
[38] Joag SV, Li Z, Foresman L, Stephens EB, Zhao LJ, Adany I, et al. Chimeric simian/human immunodeficiency virus that causes progressive loss of CD4+ T cells and AIDS in pig-tailed macaques. J Virol 1996;70:3189–97.
[39] Suryanarayana K, Wiltrout TA, Vasquez GM, Hirsch VM, Lifson JD. Plasma SIV RNA viral load determination by real-time quantification of product generation in reverse transcriptase-polymerase chain reaction. AIDS Res Hum Retroviruses 1998;14:183–9.
[40] Peek LJ, Middaugh CR, Berkland C. Nanotechnology in vaccine delivery. Adv Drug Deliv Rev 2008;60:915–28.
[41] Matsuo K, Yoshikawa T, Oda A, Akagi T, Akashi M, Okada N, et al. Efficient generation of antigen-specific cellular immunity by vaccination with poly(γ-glutamic acid) nanoparticles entrapping endoplasmic reticulum-targeted peptides. Biochem Biophys Res Commun 2007;362:1069–72.
[42] Okamoto S, Yoshii H, Akagi T, Akashi M, Ishikawa T, Okuno Y, et al. Influenza hemagglutinin vaccine with poly(γ-glutamic acid) nanoparticles enhances the protection against influenza virus infection through both humoral and cell-mediated immunity. Vaccine 2007;25:8270–8.
[43] Okamoto S, Yoshii H, Ishikawa T, Akagi T, Akashi M, Takahashi M, et al. Single dose of inactivated Japanese encephalitis vaccine with poly(γ-glutamic acid) nanoparticles provides effective protection from Japanese encephalitis virus. Vaccine 2008;26:589–94.
[44] Yoshikawa T, Okada N, Oda A, Matsuo K, Matsuo K, Mukai Y, et al. Development of amphiphilic γ-PGA-nanoparticle based tumor vaccine: potential of the nanoparticulate cytosolic protein delivery carrier. Biochem Biophys Res Commun 2008;366:408–13.
[45] Yoshikawa T, Okada N, Oda A, Matsuo K, Matsuo K, Kayamuro H, et al. Nanoparticles built by self-assembly of amphiphilic poly(γ-glutamic acid) can deliver antigens to antigen-presenting cells with high efficiency: a new tumor-vaccine carrier for eliciting effector T cells. Vaccine 2008;26:1303–13.
[46] Uto T, Wang X, Akagi T, Zenkyu R, Akashi M, Baba M. Improvement of adaptive immunity by antigen-carrying biodegradable nanoparticles. Biochem Biophys Res Commun 2009;379:600–4.
[47] Uto T, Akagi T, Hamasaki T, Akashi M, Baba M. Modulation of innate and adaptive immunity by biodegradable nanoparticles. Immunol Lett 2009;125:46–52.
[48] Okamoto S, Matsuura M, Akagi T, Akashi M, Tanimoto T, Ishikawa T, et al. Poly(γ-glutamic acid) nano-particles combined with mucosal influenza virus hemagglutinin vaccine protects against influenza virus infection in mice. Vaccine 2009;27:5896–905.
[49] Akagi T, Higashi M, Kaneko T, Kida T, Akashi M. Hydrolytic and enzymatic degradation of nanoparticles based on amphiphilic poly(γ-glutamic acid)-*graft*-L-phenylalanine copolymer. Biomacromolecules 2006;7:297–303.
[50] Imaoka K, Miller CJ, Kubota M, McChesney MB, Lohman B, Yamamoto M, et al. Nasal immunization of nonhuman primates with simian immunodeficiency virus p55gag and cholera toxin adjuvant induces Th1/Th2 help for virus-specific immune responses in reproductive tissues. J Immunol 1998;161:5952–8.
[51] Egan MA, Chong SY, Hagen M, Megati S, Schadeck EB, Piacente P, et al. A comparative evaluation of nasal and parenteral vaccine adjuvants to elicit systemic and mucosal HIV-1 peptide-specific humoral immune responses in cynomolgus macaques. Vaccine 2004;22:3774–88.
[52] Mooij P, van der Kolk M, Bogers WM, ten Haaft PJ, Van Der Meide P, Almond N, et al. A clinically relevant HIV-1 subunit vaccine protects rhesus macaques from in vivo passaged simian-human immunodeficiency virus infection. AIDS 1998;12:15–22.
[53] Earl PL, Sugiura W, Montefiori DC, Broder CC, Lee SA, Wild C, et al. Immunogenicity and protective efficacy of oligomeric human immunodeficiency virus type 1 gp140. J Virol 2001;75:645–53.
[54] Robinson Jr WE, Kawamura T, Gorny MK, Lake D, Xu JY, Matsumoto Y, et al. Human monoclonal antibodies to the human immunodeficiency virus type 1 (HIV-1) transmembrane glycoprotein gp41 enhance HIV-1 infection in vitro. Proc Natl Acad Sci USA 1990;87:3185–9.
[55] Takeda A, Robinson JE, Ho DD, Debouck C, Haigwood NL, Ennis FA. Distinction of human immunodeficiency virus type 1 neutralization and infection enhancement by human monoclonal antibodies to glycoprotein 120. J Clin Invest 1992;89:1952–7.
[56] Douek DC, Brenchley JM, Betts MR, Ambrozak DR, Hill BJ, Okamoto Y, et al. HIV preferentially infects HIV-specific CD4+ T cells. Nature 2002;417:95–8.
[57] Kiepiela P, Ngumbela K, Thobakgale C, Ramduth D, Honeyborne I, Moodley E, et al. CD8+ T-cell responses to different HIV proteins have discordant associations with viral load. Nat Med 2007;13:46–53.
[58] Staprans SI, Barry AP, Silvestri G, Safrit JT, Kozyr N, Sumpter B, et al. Enhanced SIV replication and accelerated progression to AIDS in macaques primed to mount a CD4 T cell response to the SIV envelope protein. Proc Natl Acad Sci USA 2004;101:13026–31.
[59] Tsukamoto T, Takeda A, Yamamoto T, Yamamoto H, Kawada M, Matano T. Impact of cytotoxic-T-lymphocyte memory induction without virus-specific CD4+ T-Cell help on control of a simian immunodeficiency virus challenge in rhesus macaques. J Virol 2009;83:9339–46.

JOURNAL OF VIROLOGY, May 2010, p. 4769–4781
0022-538X/10/$12.00 doi:10.1128/JVI.02279-09

Vol. 84, No. 9

Generation of the Pathogenic R5-Tropic Simian/Human Immunodeficiency Virus $SHIV_{AD8}$ by Serial Passaging in Rhesus Macaques[▽]†

Yoshiaki Nishimura,[1] Masashi Shingai,[1] Ronald Willey,[1] Reza Sadjadpour,[1] Wendy R. Lee,[1] Charles R. Brown,[1] Jason M. Brenchley,[1] Alicia Buckler-White,[1] Rahel Petros,[2] Michael Eckhaus,[3] Victoria Hoffman,[3] Tatsuhiko Igarashi,[1]‡ and Malcolm A. Martin[1]*

Laboratory of Molecular Microbiology[1] and Comparative Medicine Branch,[2] National Institute of Allergy and Infectious Diseases, and Diagnostic and Research Services Branch, Division of Veterinary Resources, Office of the Director,[3] National Institutes of Health, Bethesda, Maryland 20892

Received 28 October 2009/Accepted 31 January 2010

A new pathogenic R5-tropic simian/human immunodeficiency virus (SHIV) was generated following serial passaging in rhesus macaques. All 13 animals inoculated with $SHIV_{AD8}$ passaged lineages experienced marked depletions of $CD4^+$ T cells. Ten of these infected monkeys became normal progressors (NPs) and had gradual losses of both memory and naïve $CD4^+$ T lymphocytes, generated antiviral $CD4^+$ and $CD8^+$ T cell responses, and sustained chronic immune activation while maintaining variable levels of plasma viremia (10^2 to 10^5 RNA copies/ml for up to 3 years postinfection [p.i.]). To date, five NPs developed AIDS associated with opportunistic infections caused by *Pneumocystis carinii*, *Mycobacterium avium*, and *Campylobacter coli* that required euthanasia between weeks 100 and 199 p.i. Three other NPs have experienced marked depletions of circulating $CD4^+$ T lymphocytes (92 to 154 cells/μl) following 1 to 2 years of infection. When tested for coreceptor usage, the viruses isolated from four NPs at the time of their euthanasia remained R5 tropic. Three of the 13 $SHIV_{AD8}$-inoculated macaques experienced a rapid-progressor syndrome characterized by sustained plasma viremia of $>1 \times 10^7$ RNA copies/ml and rapid irreversible loss of memory $CD4^+$ T cells that required euthanasia between weeks 19 and 23 postinfection. The sustained viremia, associated depletion of $CD4^+$ T lymphocytes, and induction of AIDS make the $SHIV_{AD8}$ lineage of viruses a potentially valuable reagent for vaccine studies.

Simian immunodeficiency virus (SIV)/macaque models of AIDS have been extensively used as surrogates for human immunodeficiency virus type 1 (HIV-1) in studies of virus-induced immunopathogenesis and vaccine development. As is observed for the HIVs recovered from a majority of individuals during the asymptomatic phase of their infections, pathogenic SIVs utilize the CCR5 coreceptor to enter their $CD4^+$ T lymphocyte targets *in vivo* (36). This leads to the elimination of memory $CD4^+$ T cells circulating in the blood and residing at effector sites (gastrointestinal [GI] tract, mucosal surfaces, and lung), particularly during acute HIV and SIV infections (5, 29, 32, 49). In contrast to naturally occurring SIVs and HIVs, SIV/HIV chimeric viruses (simian/human immunodeficiency viruses [SHIVs]) were constructed in the laboratory by inserting a large segment of the HIV genome, including the *env* gene, into the genetic backbone of the molecularly cloned SIV_{mac239} (44). SHIVs were developed because they expressed the HIV envelope glycoprotein and could be used in vaccine experiments to evaluate neutralizing antibodies (NAbs) elicited by HIV-1 gp120 immunogens. The commonly used pathogenic SHIVs generated high levels (10^7 to 10^8 RNA copies/ml) of plasma viremia and induced an extremely rapid, systemic, and nearly complete depletion of the entire $CD4^+$ T cell population, resulting in death from immunodeficiency beginning at 3 months postinoculation (23, 26, 41). Unlike SIVs, however, these pathogenic SHIVs exclusively targeted CXCR4-expressing $CD4^+$ T cells during infections of rhesus monkeys (36). Despite their extraordinary virulence, most vaccine regimens (naked DNA, peptides, proteins, inactivated virions, recombinant modified vaccinia virus Ankara (MVA), and DNA prime/recombinant viral-vector boosting) were effective in controlling intravenous (i.v.) and mucosal X4-tropic SHIV challenges (1, 3, 33, 42, 46). When it became apparent that the same vaccination strategies that were effective in suppressing pathogenic SHIVs failed to control SIV infections, concerns were raised about whether X4 SHIVs were appropriate surrogates for HIV in vaccine experiments (13).

The unusual biological properties of the X4 SHIVs plus the discrepant outcomes of SIV and X4 SHIV vaccine experiments have become a driving force for developing CCR5-utilizing (R5) SHIVs. Although several clade B and clade C R5-tropic SHIVs have been constructed (7, 15, 21, 30, 38), the $SHIV_{SF162}$ lineage viruses are the best-characterized and most widely used R5 SHIVs (20). They have been employed in microbicide (10), neutralizing monoclonal antibody (MAb) passive-transfer (16, 17), and vaccination (2) studies.

* Corresponding author. Mailing address: Bldg. 4, Room 315A, 4 Center Drive MSC 0460, National Institutes of Health, Bethesda, MD 20892-0460. Phone: (301) 496-4012. Fax: (301) 402-0226. E-mail: malm@nih.gov.

‡ Present address: Laboratory of Primate Models, Institute for Virus Research, Kyoto University, 53 Shogoinkawaramachi, Sakyo-ku, Kyoto 606-8507, Japan.

† Supplemental material for this article may be found at http://jvi.asm.org/.

▽ Published ahead of print on 10 February 2010.

In the aftermath of the failed STEP HIV vaccine trial, there was general consensus that additional SIVs and SHIVs should be developed, particularly for use as heterologous challenge viruses in vaccine studies (12). With this goal in mind, we report the generation of a new pathogenic R5-tropic SHIV bearing the *env* gene from the HIV-1_{Ada} isolate (14). HIV-1_{Ada} was selected because it is a prototypical macrophage-tropic strain (8), uses CCR5 for cell entry (53), and has the potential for eliciting NAbs against HIV-1 gp120, and we had previously constructed a full-length infectious molecular clone (pHIV-1_{AD8}) (48). Based on previous experience in obtaining pathogenic X4-tropic SHIVs, serial passaging in macaques, treated with an anti-CD8 MAb at the time of virus inoculation, was used to expedite the adaptation of R5-SHIV sequences in a nonhuman primate host. Of the 13 animals inoculated with *in vivo*-passaged $SHIV_{AD8\#2}$ (see below) and its immediate derivatives, 10 exhibited a normal-progressor (NP) phenotype, sustaining gradual depletions of both memory and naïve $CD4^+$ T cells from the circulation and memory $CD4^+$ T cells at an effector site (lung) while maintaining variable viral-RNA loads (10^2 to 10^5 RNA copies/ml) for up to 3 years postinfection (p.i.). Five of these monkeys developed immunodeficiency with associated opportunistic infections requiring euthanasia. Three other NPs currently have total $CD4^+$ T cell counts of 92 to 154 cells/μl plasma after 1 to 2 years of infection. The remaining 3 of the 13 $SHIV_{AD8}$-inoculated macaques experienced a rapid-progressor (RP) clinical course and were euthanized between weeks 19 and 23 p.i. because of intractable diarrhea and marked weight loss. The sustained viremia, associated depletion of $CD4^+$ T lymphocytes, and induction of AIDS make the $SHIV_{AD8}$ lineage of viruses a potentially valuable reagent for vaccine studies.

MATERIALS AND METHODS

Construction of $SHIV_{AD8}$. $SHIV_{AD8}$ contains the *env* gene from the R5-tropic HIV-1_{Ada} (14)-derived molecular clone $pHIV_{AD8}$ (48). A 3.04-kb segment from $pHIV_{AD8}$, including a portion of the *vpr* gene and the entire *tat*, *rev*, *vpu*, and *env* genes, was PCR amplified using the forward primer TGAAACTTATGGGGA TACTTGGGC, which begins at nucleotide 141 of the AD8 *vpr* gene, allowing the incorporation of a unique EcoRI site, located 21 nucleotides downstream from the primer, into the PCR product. The reverse PCR primer (TCCACCCATAA GCTTATAGCAAAGTCCTTTCCAAGCCC) generated a HindIII site adjacent to and encompassing the last 2 nucleotides of the *env* reading frame, as well as a substitution of a Thr for a Leu 3 codons upstream from the *env* termination codon. PCRs were performed using 10 pmol each of the forward and reverse primers, Platinum PCR SuperMix High Fidelity (Invitrogen), and 1 μl of $pHIV_{AD8}$ in a final volume of 50 μl. The reaction mixtures were heated to 94°C for 2 min, followed by 30 cycles of 94°C for 20 s, 59°C for 30 s, and 70°C for 3 min and a 7-min extension at 70°C. The PCR product was gel extracted using a Qiaquick gel extraction kit (Qiagen) and digested with EcoRI and HindIII, and the resulting 3.04-kb restriction fragment was cloned directly into the previously described and similarly digested $pSHIV_{DH12}$ (45) to generate $pSHIV_{AD8}$. DNA sequencing of the entire 3.04-kb insert in $pSHIV_{AD8}$ was conducted to verify that no spurious changes had been introduced during the PCR amplification and cloning.

Preparation of $SHIV_{AD8}$ virus stocks. HeLa cells were transfected with 25 μg of $pSHIV_{AD8}$, and the virus present in the supernatant at 48 h was pelleted in an ultracentrifuge and resuspended in RPMI 1640 medium as previously described (52). Stocks of the cloned $SHIV_{AD8}$ were prepared by infecting PM1 cells (31) or concanavalin A (ConA)-activated rhesus monkey peripheral blood mononuclear cells (PBMC) with the HeLa-derived $SHIV_{AD8}$, as previously described (23, 24), and pooling the supernatant media at the times of peak reverse transcriptase (RT) production from both infections.

$SHIV_{AD8}$ stock 2 ($SHIV_{AD8\#2}$) was prepared from PBMC and bone marrow (BM), spleen, and lymph node (LN) samples collected from macaque CK1G on day 6 p.i. Cell suspensions from axillary, inguinal, iliac, and mesenteric LNs, PBMC, and BM were cocultivated with PBMC from uninfected animals; the culture supernatants were monitored daily for RT activity, pooled, and designated $SHIV_{AD8\#2}$. The infectious titer of $SHIV_{AD8\#2}$ was 1.5×10^3 tissue culture infective doses ($TCID_{50}$)/ml, as determined in rhesus macaque PBMC.

TABLE 1. Infection of rhesus macaques with $SHIV_{AD8\#2}$ and immediate derivatives

Animal	Inoculum
CJ8B	$SHIV_{AD8\#2}$
CK15	Blood transfusion from CJ8B (wk 60)
CJ58	Blood transfusion from CJ8B (wk 60)
CE8J	Lymph node virus[a] ($SHIV_{AD8\#2LN}$, 3.2×10^5 $TCID_{50}$) from CJ8B (wk 59)
CJ35	Lymph node virus ($SHIV_{AD8\#2LN}$, 3.2×10^5 $TCID_{50}$) from CJ8B (wk 59)
CJ3V	PBMC virus[b] ($SHIV_{AD8\#2PBMC}$, 5.9×10^4 $TCID_{50}$) from CK15 + CJ58 (wk 4)
CK5G	PBMC virus ($SHIV_{AD8\#2PBMC}$, 5.9×10^4 $TCID_{50}$) from CK15 + CJ58 (wk 4)
DB99	Blood transfusion from CJ8B (wk 117) + CK15 (wk 57) + CJ58 (wk 57)
DA1Z	Blood transfusion from CJ8B (wk 117) + CK15 (wk 57) + CJ58 (wk 57)
A4E008	Blood transfusion from DA1Z (wk 1) + DB99 (wk 1)
DA4W	Blood transfusion from DA1Z (wk 1) + DB99 (wk 1)
CL5A	$SHIV_{AD8\#2}$ passaged *in vitro* for 30 days ($SHIV_{AD8\#2.d30}$, 4.3×10^5 $TCID_{50}$)
CL98	SHIVAD8#2 passaged *in vitro* for 30 days ($SHIV_{AD8\#2.d30}$, 4.3×10^5 $TCID_{50}$)

[a] Lymph node virus: $SHIV_{AD8}$ derivative prepared from the supernatant medium collected from cocultures of lymph node suspensions plus PBMC, recovered from animal CJ8B at week 59 p.i., and PBMC from uninfected rhesus monkeys.

[b] PBMC virus: $SHIV_{AD8}$ derivative prepared from the supernatant medium collected from cocultures of PBMC, recovered from the indicated infected animals at week 4 p.i., and PBMC from uninfected rhesus monkeys.

$SHIV_{AD8}$ lymph node virus ($SHIV_{AD8LN}$) was prepared from supernatant medium collected from cocultures of lymph node suspensions plus PBMC recovered from animal CJ8B at week 59 p.i. (Table 1) and PBMC from uninfected rhesus monkeys. The infectious titer of $SHIV_{AD8LN}$ was 6.4×10^3 $TCID_{50}$/ml, as determined in rhesus macaque PBMC.

$SHIV_{AD8}$ PBMC virus ($SHIV_{AD8PBMC}$) was prepared from supernatant medium collected from cocultures of PBMC recovered and pooled from animals CK15 and CJ58 at week 4 p.i. (Table 1) and PBMC from uninfected rhesus monkeys. The infectious titer of $SHIV_{AD8PBMC}$ was 1.1×10^4 $TCID_{50}$/ml, as determined in rhesus macaque PBMC.

$SHIV_{AD8\#2.d30}$ was prepared by infecting ConA-stimulated pig-tailed macaque (PT) PBMC with $SHIV_{AD8\#2}$. Fresh ConA-stimulated PT PBMC were added to the infected cultures on days 10 and 20, and the supernatant medium collected on day 30, designated $SHIV_{AD8\#2.d30}$, had an infectious titer of 8.5×10^4 $TCID_{50}$/ml, as determined in rhesus macaque PBMC.

Virus replication assay in rhesus monkey PBMC. The preparation and infection of rhesus monkey PBMC have been described previously (25). Briefly, PBMC stimulated with concanavalin A and cultured in the presence of recombinant human interleukin-2 (IL-2) were spinoculated ($1,200 \times g$ for 1 h) (37) with virus normalized for RT activity. Virus replication was assessed by RT assay of the culture supernatant as described above.

Animal experiments. Rhesus macaques (*Macaca mulatta*) were maintained in accordance with the guidelines of the Committee on Care and Use of Laboratory Animals (9) and were housed in a biosafety level 2 facility; biosafety level 3 practices were followed. Phlebotomies, i.v. virus inoculations, euthanasia, and tissue sample collections were performed as previously described (11). Bronchoalveolar lavage (BAL) fluid lymphocytes were prepared from uninfected and infected animals using a pediatric bronchoscope (Olympus BF3C40; Olympus America, Inc., Melville, NY), as previously described (22).

Serial *in vivo* passaging of $SHIV_{AD8}$ was initiated by transferring whole blood (10 ml) and BM (2 ml) to a recipient animal previously treated with the anti-$CD8^+$ T cell-depleting MAb cM-T807 (10 mg/kg of body weight) on days −1 and +3 p.i. In subsequent passages, spleen, LN (axillary, inguinal, iliac, and mesen-

teric), PBMC, and BM cell suspensions were prepared from infected donors at the time of necropsy and transferred (1×10^8 to 3×10^8 mononuclear cells and 1×10^8 to 10×10^8 BM cells) to a new recipient by the i.v., intraperitoneal (i.p.), and BM routes.

Quantitation of proviral-DNA and plasma viral-RNA levels. The number of viral-DNA copies in PBMC was measured by quantitative DNA PCR (45). Viral-RNA levels in plasma were determined by real-time reverse transcription-PCR (ABI Prism 7700 sequence detection system; Applied Biosystems, Foster City, CA) as previously reported, using reverse-transcribed viral RNA in plasma samples from SIV_{mac239}-inoculated rhesus macaques (11).

Lymphocyte immunophenotyping and data analysis. EDTA-treated blood samples and BAL fluid lymphocytes were stained for flow cytometric analysis as described previously (34, 36), using combinations of the following fluorochrome-conjugated MAbs: CD3 (fluorescein isothiocyanate [FITC] or phycoerythrin [PE]), CD4 (PE, peridinin chlorophyll protein-Cy5.5 [PerCP-Cy5.5], or allophycocyanin [APC]), CD8 (PerCP or APC), CD28 (FITC or PE), CD95 (APC), and Ki-67 (FITC or PE). All antibodies were obtained from BD Biosciences (San Diego, CA), and samples were analyzed by four-color flow cytometry (FACSCalibur; BD Biosciences Immunocytometry Systems). Data analysis was performed using CellQuest Pro (BD Biosciences) and FlowJo (TreeStar, Inc., San Carlos, CA). For Ki-67 staining, cells were fixed with fluorescence-activated cell sorter (FACS) lysing solution (Becton Dickinson), treated with FACS permeabilization buffer 2 (Becton Dickinson), and stained with Ki-67 MAb or a control isotype IgG1. In this study, naïve $CD4^+$ T cells were identified by their $CD95^{low}$ $CD28^{high}$ phenotype, whereas memory $CD4^+$ T cells were $CD95^{high}$ $CD28^{high}$ or $CD95^{high}$ $CD28^{low}$ in the $CD4^+$ small lymphocyte gate (36, 39).

Intracellular-cytokine assays. Stimulation was performed on frozen lymphocytes as described previously (40). Freshly thawed lymphocytes were resuspended (10^6/ml) in RPMI medium supplemented with antibiotics and glutamine. Anti-CD28 conjugated to Alexa 594-PE was used for costimulation. Staphylococcus enterotoxin B (1 μg/ml; Sigma-Aldrich, St. Louis, MO) was used to stimulate T cells mitogenically through the T cell receptor as a positive control. A negative control (cells treated only with costimulatory anti-CD28) was included in every experiment. Peptides used to stimulate SIV-specific T cells were 15 amino acids (aa) in length, overlapping by 11 amino acids, and encompassed SIV_{mac239} Gag (New England Peptide, Gardner, MA). The concentration of each peptide was 2 μg/ml for stimulations, which were performed in the presence of brefeldin A (BFA) (1 μg/ml; Sigma-Aldrich, St. Louis, MO) for 16 h at 37°C. All cells were surface stained with the dead-cell exclusion dye Aqua Blue (Invitrogen Corp., Carlsbad CA), followed by staining with anti-CD3 Alexa 700 (BD Biosciences), anti-CD4 Cy5.5-PE (eBioscience Inc., San Diego, CA), anti-CD8 Pacific Blue (BD Biosciences), and anti-CD95 Cy5-PE (BD Biosciences). The cells were then fixed, permeabilized, and stained with anti-gamma interferon (IFN-γ) Cy7-PE (BD Biosciences), anti-IL-2 APC (BD Biosciences), tumor necrosis factor (TNF) FITC (BD Biosciences), and Mip1-β PE (BD Biosciences). SIV-specific CD8 T cell responses are reported as the frequency of memory CD8 T cells, gated by characteristic light scatter properties; then as Aqua $Blue^-$, $CD3^+$, $CD8^+$, $CD4^-$, or $CD95^+$; and by production of either TNF or Mip-1β. All data are reported after background subtraction.

Virus neutralization assays. Autologous plasma samples (1:20 dilution) from $SHIV_{AD8}$-infected macaques were incubated with (i) the same uncloned $SHIV_{AD8}$ derivative used for inoculation or (ii) the $SHIV_{AD8}$ isolated from PBMC at week 4 p.i. (for monkeys CJ58 and CK15) in quadruplicate in 96-well flat-bottom culture plates in a total volume of 50 μl for 1 h at 37°C. Prechallenge plasma samples from each animal served as controls. Freshly trypsinized TZM-bl cells (50) (1.5×10^4 in 150 μl Dulbecco's modified Eagle's medium [DMEM] containing 20 μg/ml DEAE dextran) were added to each well, and the cultures were maintained in a 37°C incubator for 28 h. The amount of virus-induced luciferase activity, measured as relative light units (RLU), present in cell lysates was determined as previously described (51), and the average neutralization activity for each plasma sample was determined. The average number of RLU for the prechallenge plasma controls ranged from 1×10^5 to 2×10^5. Any sample resulting in a 50% reduction of luciferase activity compared to that obtained with the uninfected control sample was considered positive for NAbs. To determine neutralizing-antibody titers, 40 μl of diluted virus, sufficient to generate the desired numbers of RLU, was mixed with 10 μl of appropriately diluted plasma samples in a 96-well plate and incubated for 1 h at 37°C. TZM-bl cells were added, cultures were maintained for an additional 28 h, and intracellular luciferase activity was measured as described above.

Coreceptor utilization assays. Freshly trypsinized TZM-bl cells (1×10^4 per well) in 135 μl DMEM containing 10% fetal calf serum (FCS) and DEAE dextran (15 μg/ml) were seeded in flat-bottom 96-well plates. Twenty-five microliters of coreceptor antagonists (AD101 against CCR5, AMD3100 against CXCR4, or both, at final concentrations ranging from 0.1 nM to 1,000 nM) was added to each well. Following incubation for 1 h at 37°C, 10 $TCID_{50}$ of replication-competent virus, determined in TZM-bl cells as previously described, in 40 μl was added to each well. After 24 h of incubation at 37°C, luciferase activity was determined. The percent infectivity reported was derived from the mean of quadruplicate assays.

To generate 293T cell-derived $SHIV_{AD8}$ pseudotyped viruses, two separate plasmids were constructed. The first (pNLenv1) contained a frameshifted mutation in the leader peptide region of gp120 (43). Plasmids expressing the $SHIV_{AD8(RIG+)}$ and $SHIV_{AD8(RIG-)}$ *env* genes [pCMV-AD8(RIG+) and AD8(RIG−)] were generated by reverse transcription-PCR of plasma viral RNA, collected from macaque DB99 at the time of euthanasia, and subcloning into NotI and (newly created) XbaI sites of the pCMVbeta expression plasmid (Clonetech, Palo Alto, CA). Both plasmids [pNLenv1 and pCMV-AD8(RIG) in a 5:1 ratio] were cotransfected into 293T cells using Lipofectamine 2000 (Invitrogen, Carlsbad, CA). The titers of pseudotyped-virus preparations were determined, and they were assayed for coreceptor usage 48 h following infection of TZM-bl cells, as described for replication-competent virus.

RESULTS

Construction of a CCR5-tropic SHIV. We previously reported the construction of a full-length infectious HIV-1 molecular clone ($pHIV\text{-}1_{AD8}$) derived from the prototypical macrophage-tropic CCR5-utilizing $HIV\text{-}1_{Ada}$ isolate (14, 48). A SHIV expressing the *env* gene from $pHIV_{AD8}$ was obtained by inserting the 3.04-kb EcoRI-to-HindIII DNA fragment (including a portion of *vpr* and the entire *tat*, *rev*, *vpu*, and *env* genes) into the genetic background of $pSHIV_{DH12}$ (45), as described in Materials and Methods. The resulting molecular clone, $pSHIV_{AD8}$, directed the production of progeny virions following the transfection of HeLa cells. Virus stocks were prepared by infecting PM1 cells or ConA-stimulated rhesus PBMC with virions pelleted from HeLa cell transfection culture supernatants.

It is not generally appreciated how daunting it is to generate an R5-tropic SHIV able to maintain detectable levels of set-point viremia, exclusively target memory $CD4^+$ T cells, and induce immunodeficiency in inoculated rhesus monkeys. Simply replacing orthologous SIV sequences with a DNA segment including a CCR5-utilizing HIV-1 *env* gene does not usually result in a SHIV exhibiting robust replication kinetics *in vivo* and a disease-inducing phenotype. This was, in fact, the case for $SHIV_{AD8}$: levels of plasma viremia following virus inoculation (1 ml of undiluted virus by the i.v., i.p., and BM routes) were promptly and durable suppressed, and the numbers of memory $CD4^+$ T lymphocytes did not change appreciably, as shown for a representative infected animal (CJ7H) in Fig. 1a. To be certain that we were on the right track with respect to the targeting and elimination of memory, not naïve, $CD4^+$ T cells *in vivo*, a second macaque (CJ9F) was treated with the $CD8^+$ T lymphocyte-depleting MAb cM-T807 24 h prior to $SHIV_{AD8}$ inoculation, as well as on days 3 and 6 post-virus infection, to promote a vigorous *in vivo* infection. Unlike untreated macaque CJ7H, the levels of plasma viral RNA in monkey CJ9F rapidly rose to 3.8×10^7 copies/ml by day 10 p.i. and were associated with a rapid and irreversible decline of circulating memory $CD4^+$ T cells (Fig. 1b). In contrast, the numbers of naïve $CD4^+$ T lymphocytes in animal CJ9F were maintained in the 600- to 800-cell/μl range during this period. This result, therefore, confirmed that $SHIV_{AD8}$ could sustain high virus loads and preferentially target the memory $CD4^+$ T

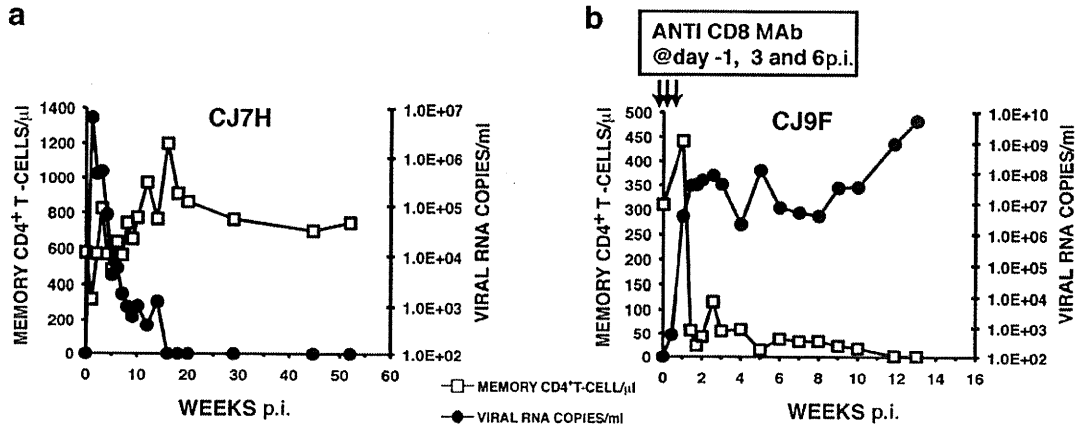

FIG. 1. Infectivity of the original $SHIV_{AD8}$ in rhesus monkeys. Macaques CJ7H (a) and CJ9F (b) were inoculated with 1 ml of undiluted $SHIV_{AD8}$ by the i.v., i.p., and BM routes. Macaque CJ9F was treated with the depleting anti-CD8 MAb cM-T807 as indicated.

cell subset *in vivo*, but only in an animal with a compromised immune system.

***In vivo* passaging of $SHIV_{AD8}$.** The prompt control of plasma viremia and the nonpathogenic phenotype of $SHIV_{AD8}$ observed in untreated macaques were reminiscent of the infectivity patterns observed with first-generation X4-tropic SHIVs (28, 44). We therefore initiated serial animal-to-animal passaging of $SHIV_{AD8}$ with macaque CJ9F as the "founder" infected monkey (Fig. 2a). This approach had previously been used to generate X4 SHIVs exhibiting more robust replicative and pathogenic properties (26, 41). Unfortunately, *in vivo* serial passaging of virus to optimize infectivity is an empirical and stochastic process. One never knows when or if an R5 SHIV has acquired an augmented replicative phenotype. The ultimate proof that such a change has occurred requires the inoculation of additional animals and waiting several months to assess the resultant viral replication kinetics and $CD4^+$ T cell dynamics.

The strategy employed was to maximize the emergence of disease-inducing SHIV variants, putatively present in an increasingly genetically diverse virus population, by serially transferring large numbers of infected cells by i.v., i.p., and BM routes into recipient animals previously treated with an anti-CD8 depleting MAb. As indicated in Fig. 2a, whole blood and bone marrow cells were transferred from macaque CJ9F to macaque H681 by these three routes. In subsequent passages, cell suspensions were prepared from spleen, LN (axillary, inguinal, iliac, and mesenteric), PBMC, and BM cells collected at the time of necropsy, as described in Materials and Methods. With one exception (macaque CJ7F), the depleting anti-CD8 MAb was administered to a recipient animal on days −1 and +3 p.i. to facilitate unrestricted replication *in vivo*. Animal CJ7F did not receive anti-CD8 MAb at the time of virus transfer to investigate the possibility that $SHIV_{AD8}$ had acquired improved replication properties *in vivo* following the initial two *in vivo* passages. Because this was not the case (its plasma viral-RNA loads had declined to 360 RNA copies/ml at week 10 p.i.), macaque CJ7F was treated with anti-CD8 MAb at week 13 p.i. and sustained an immediate burst of virus production that reached 1.4×10^6 RNA copies/ml of plasma at week

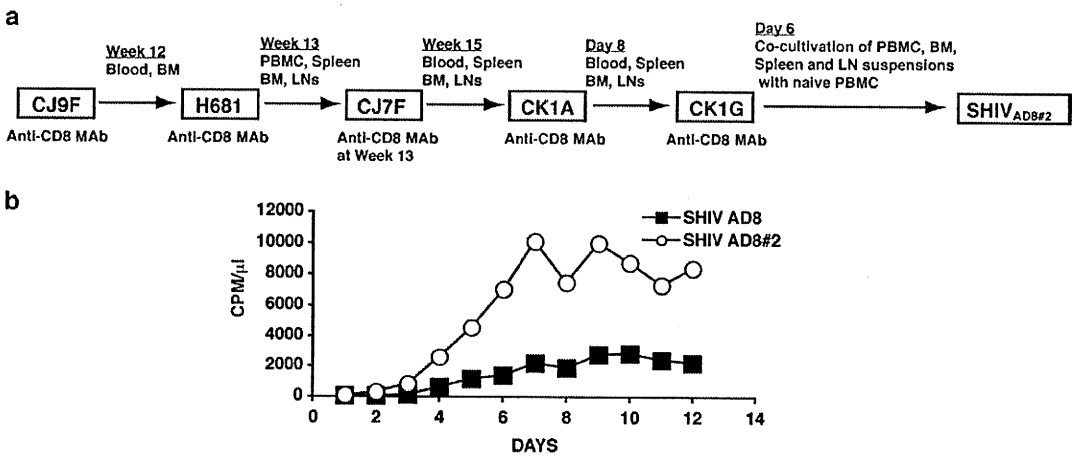

FIG. 2. Serial animal-to-animal passage of $SHIV_{AD8}$. (a) Passage history of $SHIV_{AD8}$ and origin of $SHIV_{AD8\#2}$. (b) Rhesus monkey PBMC were infected with $SHIV_{AD8}$ or the passaged $SHIV_{AD8\#2}$ virus stock, normalized for RT activity. CPM, counts per minute.

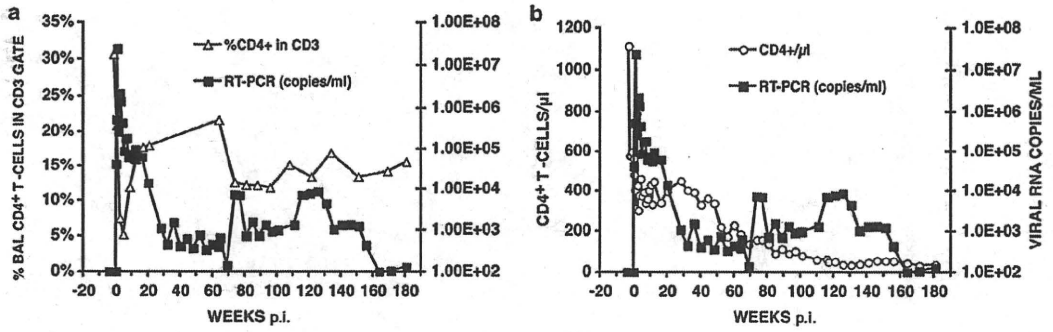

FIG. 3. $SHIV_{AD8\#2}$ induces sustained plasma viremia and loss of CD4 T cells in an inoculated rhesus macaque. Plasma viremia and the percentage of BAL fluid $CD4^+$ T cells (a) or the absolute numbers of circulating $CD4^+$ T cells (b) in rhesus macaque CJ8B inoculated intravenously with $SHIV_{AD8\#2}$ are shown. RT-PCR, reverse transcription-PCR.

14 p.i. CJ7F was euthanized at week 15 p.i., and cell suspensions were prepared as described above and transferred by the i.v., i.p., and BM routes into macaque CK1A, previously treated with anti-CD8 MAb (Fig. 2a). Following the fifth *in vivo* passage, macaque CK1G was euthanized on day 6 p.i., and cell suspensions, prepared at the time of necropsy, were cocultivated with ConA-stimulated PBMC from uninfected rhesus monkeys as described in Materials and Methods; the culture supernatants were monitored for the presence of reverse transcriptase activity, pooled, and designated $SHIV_{AD8\#2}$.

Inoculation of rhesus macaques with $SHIV_{AD8\#2}$ and its immediate derivatives resulted in sustained plasma viremia and loss of $CD4^+$ T lymphocytes. To ascertain whether serial passaging of $SHIV_{AD8}$ *in vivo* had resulted in the acquisition of improved replicative properties, ConA-stimulated rhesus monkey PBMC were infected with $SHIV_{AD8\#2}$ or the starting $SHIV_{AD8}$ virus preparation, both normalized for RT activity. As shown in Fig. 2b, $SHIV_{AD8\#2}$ replicated to much higher levels in cultured macaque PBMC than the original $SHIV_{AD8}$. To determine whether this improved infectivity of $SHIV_{AD8\#2}$ for rhesus PBMC was correlated with augmented replication in an animal not treated with the depleting anti-CD8 MAb, macaque CJ8B was inoculated i.v. with 1.5×10^4 $TCID_{50}$ of $SHIV_{AD8\#2}$. As shown in Fig. 3a, this monkey experienced a marked but transient depletion of memory $CD4^+$ T cells in BAL specimens during the acute infection and maintained detectable levels of plasma viremia. Because animal CJ8B subsequently experienced a decline in the total circulating $CD4^+$ T lymphocyte population from 565 to 175 cells/µl at week 56 p.i. (Fig. 3b), whole blood or virus propagated ex vivo from CJ8B lymph node suspensions (lymph node virus [$SHIV_{AD8LN}$]) was inoculated into four additional macaques (CK15, CJ58, CE8J, and CJ35) (Fig. 4). Four other animals (DB99, DA1Z, A4E008, and DA4W) received blood transfusions, and two (CJ3V and CK5G) were inoculated with PBMC coculture virus ($SHIV_{AD8PBMC}$) derived from monkeys CK15 and CJ58 (Fig. 4). In addition, because it was unknown at the time of its preparation whether $SHIV_{AD8\#2}$ had acquired augmented *in vivo* infectivity properties, $SHIV_{AD8\#2}$ was propagated for an additional 30 days *ex vivo* in macaque PBMC as described in Materials and Methods. Because the resulting derivative, designated $SHIV_{AD8\#2.d30}$, exhibited robust infectivity in both pigtailed and rhesus macaque PBMC (data not shown), it was inoculated intravenously into two rhesus monkeys (CL5A and CL98) (Fig. 4). The inocula used to infect rhesus monkeys with $SHIV_{AD8\#2}$ and its immediate derivatives are listed in Table 1. None of these monkeys received the depleting anti-CD8 MAb.

Ten of the 13 animals infected with $SHIV_{AD8\#2}$ or its immediate derivatives experienced an NP clinical course characterized by set-point virus loads that varied widely (from less than 10^3 to more than 10^5 RNA copies/ml) and a gradual depletion of circulating $CD4^+$ T lymphocytes (Fig. 5a and b). Transient, and in some cases quite significant, losses of memory $CD4^+$ T cells in BAL samples was a common finding during the acute infection (Fig. 5c). The loss of circulating $CD4^+$ T lymphocytes in the 10 $SHIV_{AD8\#2}$-infected NPs affected both memory and naïve subsets (Fig. 6). With one exception (monkey CJ35), these animals sustained depletions of circulating memory $CD4^+$ T cells to the 200-cell/µl level by week 100. NPs also experienced increased memory $CD4^+$ T lymphocyte turnover, as monitored by Ki-67 expression, particularly during the first 10 weeks and the final stages of the infection (see Fig. S1 in the supplemental material). The loss of naïve $CD4^+$ T lymphocytes in NP monkeys was even more profound. By week 80 p.i., this subset had declined to below 100 cells/µl in all of the animals (Fig. 6b). At the time of their euthanasia, five NPs (CJ8B, CE8J, CJ3V, CK15, and CL98) had only 1, 3, 6, 12, and 68 circulating naïve $CD4^+$ T cells/µl, respectively. We previously reported that SIVsmE543-infected

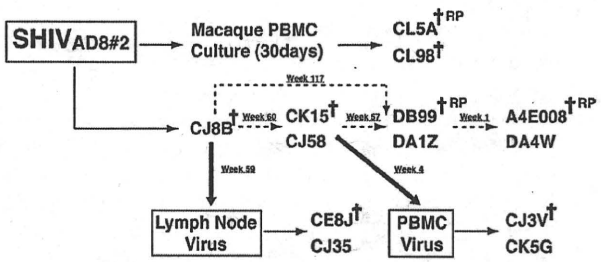

FIG. 4. $SHIV_{AD8\#2}$ and its immediate derivatives cause immunodeficiency in rhesus macaques. The dashed arrows indicate virus transfer by blood transfusion. The thick arrows indicate LN or PBMC specimens used to generate virus stocks by coculturing with PBMC from uninfected donors. †, euthanized animals.

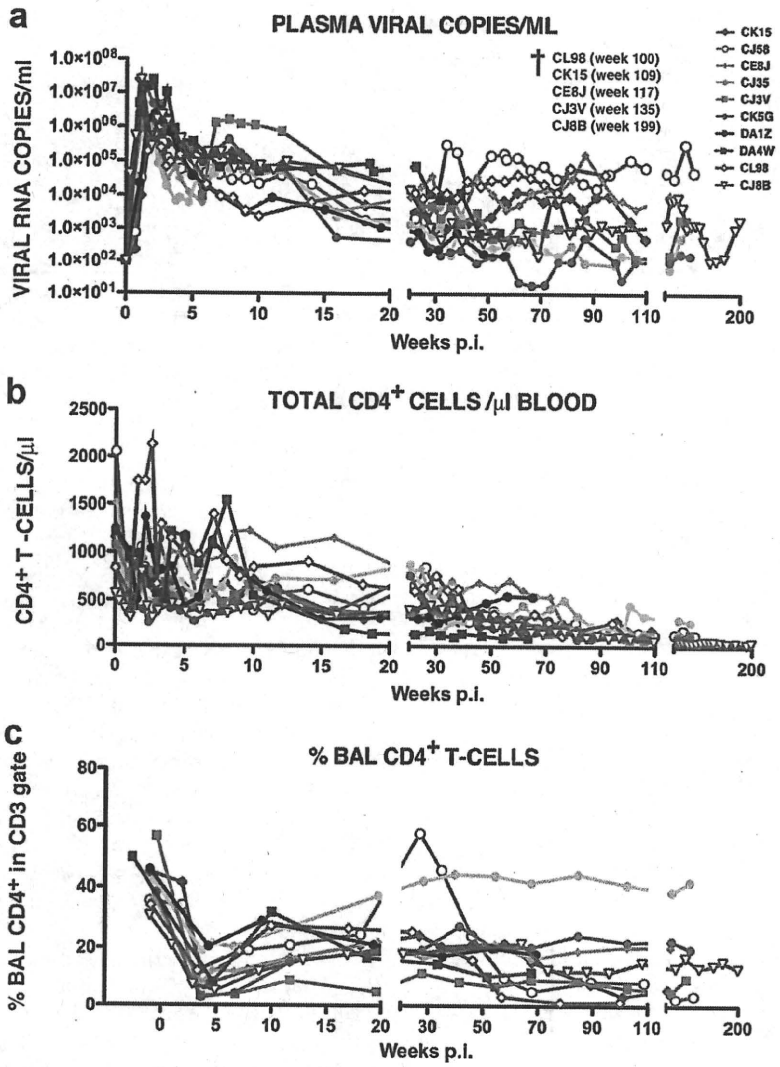

FIG. 5. Total $CD4^+$ T lymphocytes are gradually lost in normal progressors following infection with $SHIV_{AD8\#2}$ and its immediate derivatives. The levels of plasma viremia (a), absolute numbers of peripheral $CD4^+$ T cells (b), and percentages of BAL fluid $CD4^+$ T cells (c) are shown. The five normal progressors that developed AIDS and were euthanized are indicated (†).

NPs had also experienced a marked loss of naïve $CD4^+$ T cells as early as 20 weeks p.i. (35). It was therefore not unexpected that NP $SHIV_{AD8}$-infected monkeys might also sustain a depletion of their naïve $CD4^+$ T cell subset.

Three of the 13 macaques inoculated with $SHIV_{AD8\#2}$ and its immediate derivatives became RPs, requiring euthanasia between weeks 19 and 23 p.i. because of anorexia, intractable diarrhea, and marked weight loss (Fig. 7). Virus set points in the RPs exceeded 10^7 RNA copies/ml, memory $CD4^+$ T cells in BAL specimens rapidly and irreversibly declined, and at the time of death, all of the animals had sustained marked losses of circulating $CD4^+$ T cells.

Immune responses to $SHIV_{AD8}$. In the context of its use as a challenge virus in vaccine experiments, it was important to show that $SHIV_{AD8}$ elicited both cellular and humoral immune responses during infections of rhesus monkeys. Therefore, anti-$SHIV_{AD8}$ Gag-specific $CD8^+$ T lymphocyte responses were measured by flow cytometry for 6 of the 10 NPs by intracellular staining of cells expressing TNF-α and/or IFN-γ following stimulation with a 15-mer peptide pool spanning SIV_{mac239} Gag. The levels of virus-specific $CD8^+$ T cells in this group of rhesus monkeys ranged from 0.33 to 1.68% during the second year of their infection (see the table in the supplemental material). A similar analysis of Gag-specific responses in memory $CD4^+$ T cells at these times in the same animals indicated that 0.90 to 2.90% expressed TNF-α and/or IFN-γ (see the table in the supplemental material).

NAbs were detected in several of the NPs during the course of their infections (Fig. 8). The seven macaques evaluated had been inoculated with $SHIV_{AD8\#2}$ or two immediate derivatives ($SHIV_{AD8\#2LN}$ and $SHIV_{AD8\#2PBMC}$). Plasma neutralizing activity directed against the same virus used for animal challenge was evaluated in monkeys CJ8B, CE8J, CJ35, CJ3V, and

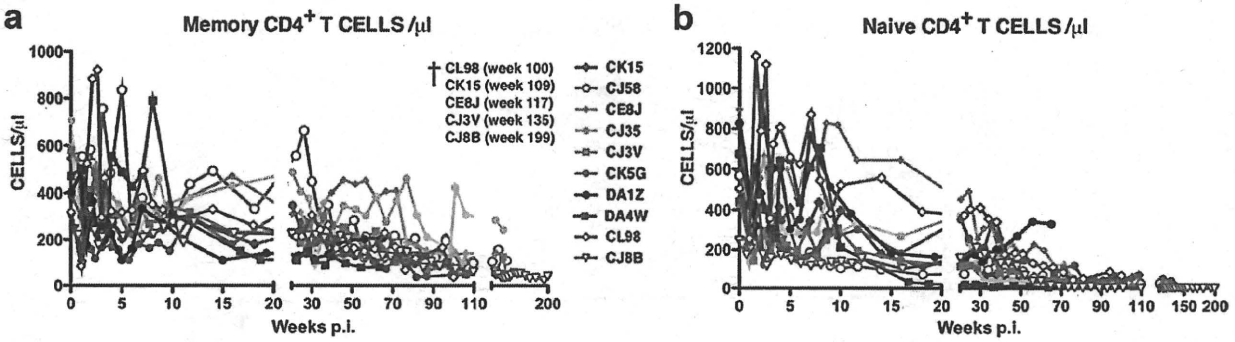

FIG. 6. Marked depletion of naïve and memory CD4$^+$ T lymphocytes characterizes long-term SHIV$_{AD8}$ infection in NP rhesus monkeys. Absolute numbers of memory CD4$^+$ T cells (a) and naive CD4$^+$ T cells (b) in 10 normal-progressor macaques during 200 weeks of SHIV$_{AD8}$ infection are shown. †, euthanized animals.

CK5G. The neutralization sensitivity of autologous virus (SHIV$_{AD8\#2PBMC}$) was monitored using plasma collected from PBMC of macaques CK15 and CJ58 (Fig. 4). The time of appearance of neutralization activity varied widely (week 20 to week 78 p.i.) and was generally correlated with levels of set-point viremia. In the three macaques producing the highest levels of anti-SHIV$_{AD8}$ NAbs, the actual 50% inhibitory concentration (IC$_{50}$) neutralization titers determined by limiting plasma dilution were 1:159 (CJ8B at week 89), 1:102 (CJ58 at week 30), and 1:143 (CE8J at week 52).

Coreceptor usage by SHIV$_{AD8}$ lineage viruses. The *env* gene of SHIV$_{AD8}$ was derived from the prototypical macrophage-tropic HIV-1$_{Ada}$, previously shown to use CCR5 for cell entry (53). When tested in a TZM-bl entry assay with inhibitors that specifically target CXCR4 or CCR5, the original SHIV$_{AD8}$, SHIV$_{AD8\#2}$ (data not shown), and SHIV$_{AD8\#2LN}$ exclusively utilized CCR5 (see Fig. S2 in the supplemental material). The marked depletion of circulating naïve CD4$^+$ T cells in all SHIV$_{AD8}$ NPs (Fig. 6b) raised the possibility that a coreceptor switch had occurred, enabling these viruses to enter and eliminate naïve CD4$^+$ T cells, which express high levels of surface CXCR4, but not CCR5. Accordingly, virus was recovered from three NPs (CK15, CE8J, and CL98) immediately prior to euthanasia. When tested for coreceptor usage, the viruses isolated from all three NPs remained R5 tropic (see Fig. S2 in the supplemental material), indicating that the loss of naïve CD4$^+$ T cells was not due to direct virus-induced cell killing.

As noted earlier, three monkeys infected with SHIV$_{AD8\#2}$ derivatives exhibited an RP phenotype. By week 10 p.i., these macaques (DB99, A4E008, and CL5A) had experienced massive loss of memory CD4$^+$ T cells in samples collected by BAL (Fig. 7c) but had little change in the number of circulating naive CD4$^+$ T lymphocytes (data not shown). However, by week 19 p.i., the levels of total CD4$^+$ T cells in the blood had declined significantly in all three RPs (Fig. 7b), raising again the possibility that coreceptor usage might have changed. To assess a possible coreceptor switch, virus was collected from RP monkeys DB99 and A4E008 at the time of euthanasia and evaluated in the TZM-bl assay with specific CXCR4 and CCR5 inhibitors. As shown in Fig. 9a, blocking the entry of SHIV$_{AD8\text{-}DB99}$ required both inhibitors, whereas SHIV$_{AD8\text{-}A4E008}$ was inhibited only by the CCR5 inhibitor. This result indicates that SHIV$_{AD8\text{-}DB99}$ had acquired the capacity to use CXCR4 during its infection of macaque DB99 and that SHIV$_{AD8\text{-}A4E008}$ had remained R5 tropic.

Reverse transcription-PCR cloning and sequencing of *env* genes amplified from the plasma of macaque DB99 at the time of its euthanasia revealed that 28 of 29 recovered clones contained a 3-aa insertion (RIG) located 2 residues upstream of the GPGR sequence in the crown of the gp120 V3 region (Fig. 9b). A similar analysis of the *env* gene from virus circulating in monkey A4E008 revealed a different 3-aa insertion (HIG) at the same location in its V3 loop. The V3 loop sequences amplified from the plasma of both animals at week 2 p.i. did not contain any insertion. The gp120 region amplified from the third RP (macaque CL5A) at the time of euthanasia contained no insertion (Fig. 9b).

One of the 28 viral-DNA clones amplified from macaque DB99 plasma at the time of euthanasia containing the RIG insertion in V3 and the single clone simultaneously obtained from this animal lacking the V3 insertion were used to prepare pseudotyped virus for testing in the entry assay, as described in Materials and Methods. As shown in Fig. 9c, the V3 RIG insertion conferred usage of both CCR5 and CXCR4 coreceptors on SHIV$_{psAD8(RIG+)}$ compared to the exclusive utilization of CCR5 by SHIV$_{psAD8(RIG-)}$, which lacks the gp120 V3 insertion.

SHIV$_{AD8}$-infected macaques developed immunodeficiency. The clinical statuses and disease outcomes of all 13 animals inoculated with SHIV$_{AD8\#2}$ and its immediate derivatives during a 2- to 3-year observation period are presented in Table 2. As noted above, 10 of these 13 macaques were NPs and experienced gradual and irreversible depletions of both memory and naïve CD4$^+$ T lymphocyte subsets (Fig. 6). Five of these animals were euthanized with symptoms of AIDS, and 3 additional NPs currently have CD4$^+$ T cell counts ranging from 92 to 154 cells/μl plasma (Table 2). Histopathological studies performed on specimens collected at the time of necropsy revealed the presence of *Pneumocystis carinii*, *Mycobacterium avium*, and *Campylobacter coli* infections in individual macaques (see Fig. S3 in the supplemental material). In addition, 3 of the 13 R5-SHIV-infected monkeys experienced an RP syndrome characterized by sustained plasma viremia of

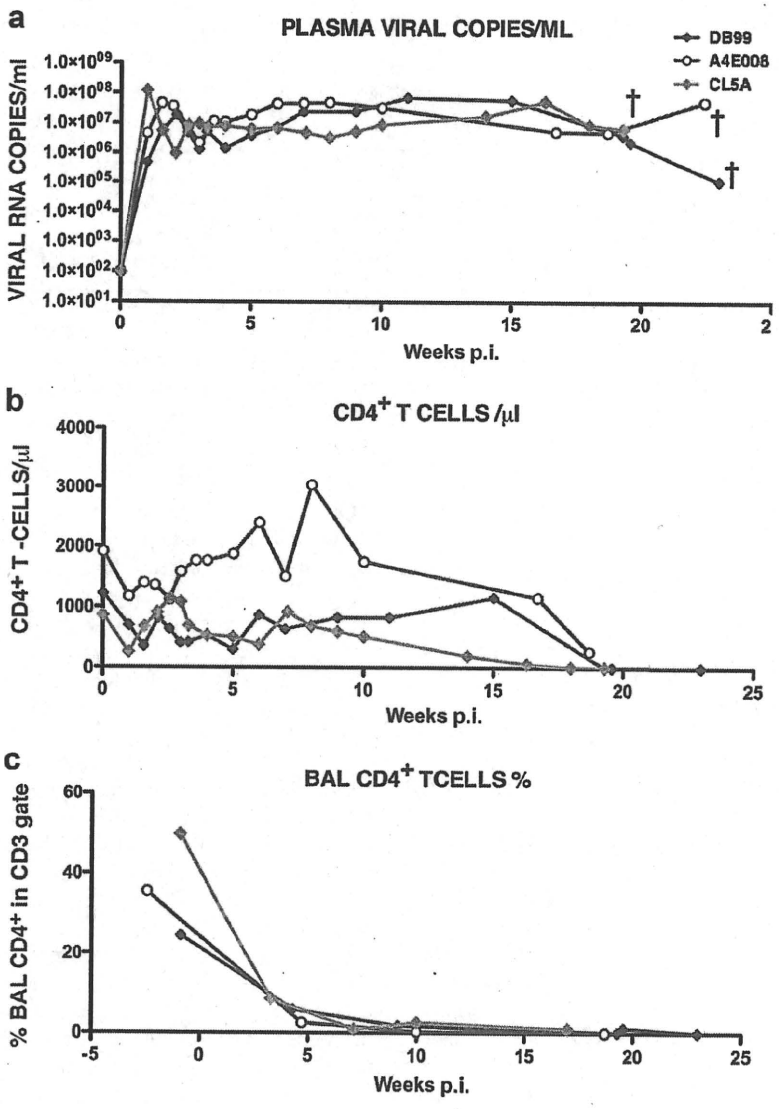

FIG. 7. Patterns of virus replication and CD4+T cell dynamics in $SHIV_{AD8}$ rapid progressors. The levels of plasma viremia (a), absolute numbers of peripheral $CD4^+$ T cells (b), and percentages of BAL fluid $CD4^+$ T cells (c) are shown. †, euthanized animals.

$>1 \times 10^7$ RNA copies/ml; rapid and irreversible loss of memory $CD4^+$ T cells in the blood and at an effector site (BAL); and intractable diarrhea, anorexia, and weight loss requiring euthanasia between weeks 19 and 23 p.i.

DISCUSSION

The results presented clearly show that the generation of a pathogenic R5-SHIV was not a trivial undertaking. Animal-to-animal passaging eventually gave rise to $SHIV_{AD8\#2}$, possessing greatly augmented infectivity for rhesus PBMC compared to the starting $SHIV_{AD8}$ construct. Although it was not appreciated at the time, $SHIV_{AD8\#2}$ had also acquired improved *in vivo* properties, as evidenced by its and its immediate derivatives' capacity to cause fatal immunodeficiency in 8 of 13 inoculated rhesus monkeys (Fig. 4 and Table 2). The most consistent and distinguishing property of the passaged $SHIV_{AD8}$ family of viruses during infections of rhesus macaques was the slow and unremitting loss of both memory and naïve $CD4^+$ T cells (Fig. 6), a pattern of depletion observed in all 10 NPs. Surprisingly, and in contrast to both SIVmac and SIVsmE lineages, the pace of $CD4^+$ T lymphocyte decline was not correlated with plasma virus loads. Although the geometric mean plasma viral-RNA level at week 50 in the $SHIV_{AD8}$-infected monkey cohort was 1.7×10^3 RNA copies/ml, the set-point virus loads varied widely in the 10 infected animals

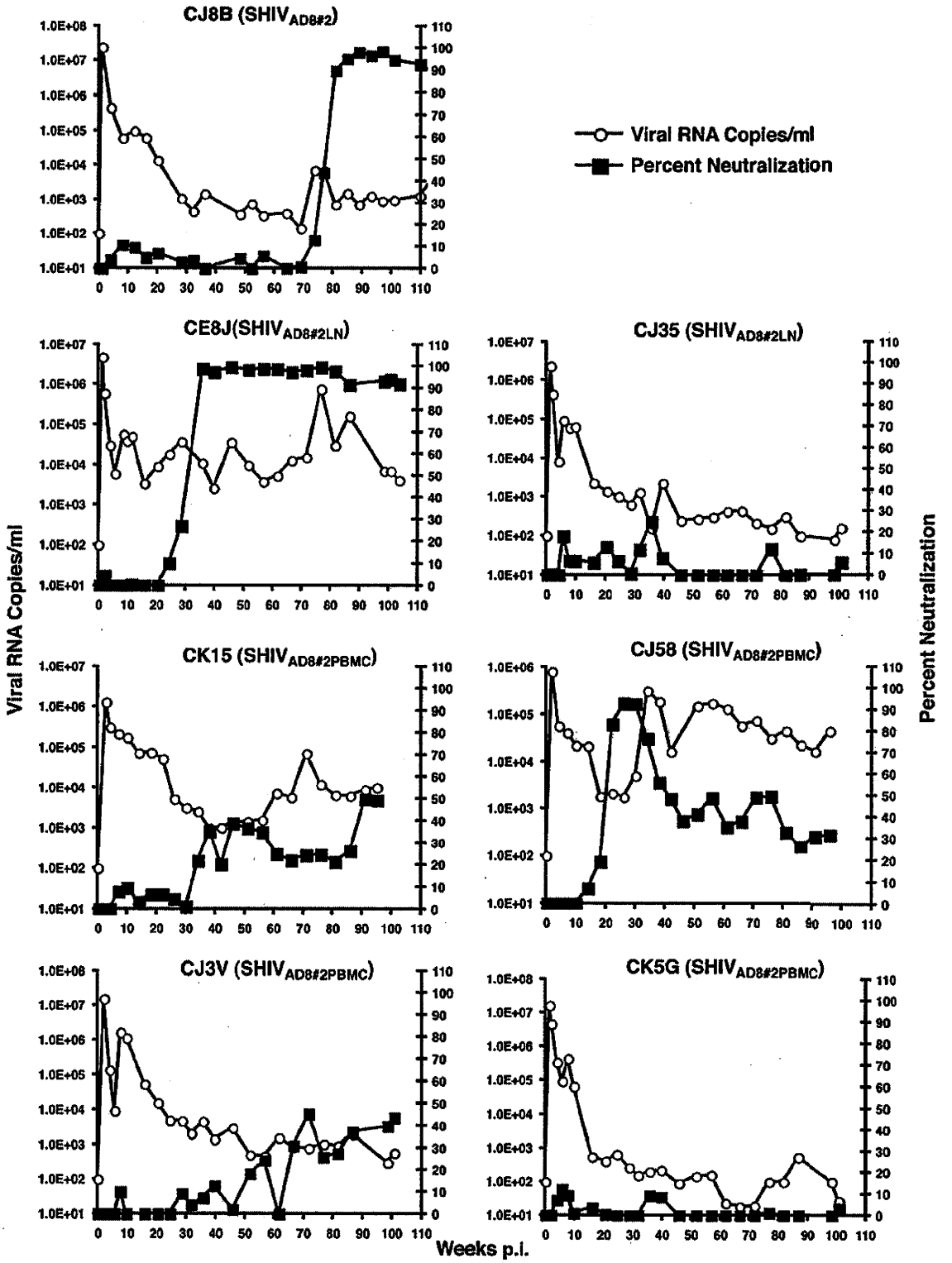

FIG. 8. Neutralizing-antibody activities detected in normal-progressor macaques following infection with SHIV$_{AD8\#2}$ or its immediate derivatives. Plasma samples (1:20 dilution) from the indicated SHIV$_{AD8}$-infected macaques were incubated in quadruplicate for 1 h at 37°C with the virus isolates shown in parentheses and then used as an inoculum to infect TZM-bl cells. The luciferase activity present in cell lysates at 28 h p.i. was measured, and the average percent neutralization activity in plasma at each time point was determined. Prechallenge plasma samples served as negative controls and baselines for zero neutralizing-antibody activity.

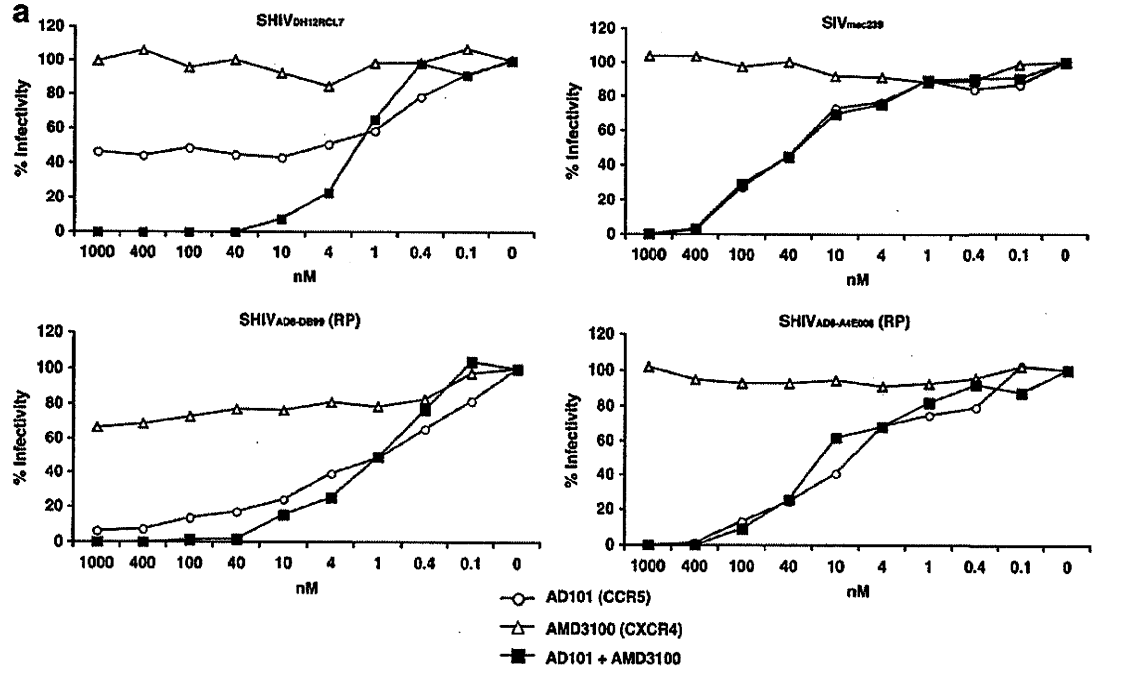

b

VIRUS		N-TERMINAL V3 STEM	CORECEPTOR USAGE
$SHIV_{AD8}$		NNTRKSI---HI--GPGR	CCR5
$SHIV_{AD8\text{-}DB99}$	Rapid Progressor	NNTRKSIRIGHI--GPGR	CXCR4/CCR5
$SHIV_{AD8\text{-}A4E008}$	Rapid Progressor	NNTRKSIHIGHI--GPGR	CCR5
$SHIV_{AD8\text{-}CL5A}$	Rapid Progressor	NNTRKSI---HI--GPGR	(Undetermined)
$SHIV_{162P3}$		NNTRKSI---TI---GPGR	CCR5
$SHIV_{162\text{-}BR24N}$	Rapid Progressor	NNTRKSI---TIHRGPGR	CXCR4

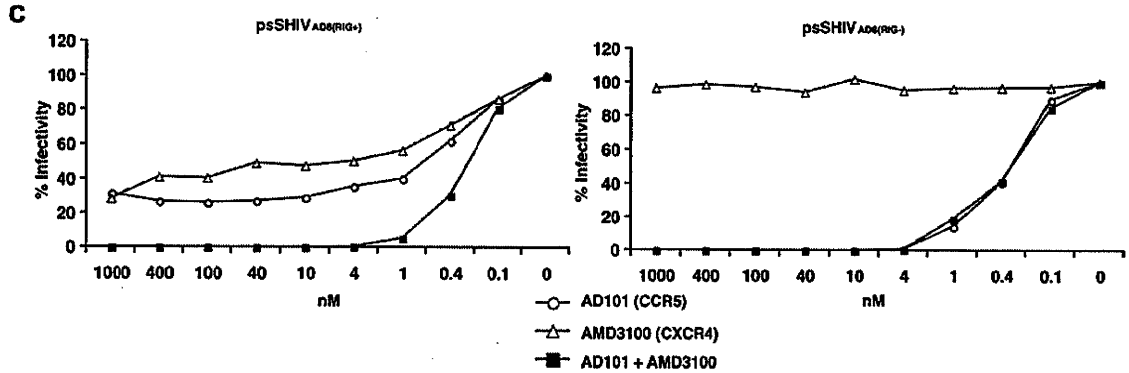

FIG. 9. Coreceptor utilization of $SHIV_{AD8}$ derivatives isolated from rapid progressors. (a) TZM-bl cells were infected in quadruplicate with viruses ($SHIV_{AD8\text{-}DB99}$ and $SHIV_{AD8\text{-}A4E008}$) recovered from rapid progressors DB99 and A4E008, respectively, in the presence of the indicated amounts of the small-molecule coreceptor inhibitors AD101 (CCR5), AMD 3100 (CXCR4), or both. SIV_{mac239} and $SHIV_{DH12RCL\text{-}7}$ were also analyzed as representative R5-tropic and dual-tropic viruses, respectively. The luciferase activities present in cell lysates 24 h p.i. were measured, and percent infectivities were determined in the absence or presence of coreceptor inhibitors. (b) gp120 sequences from the N-terminal V3 regions of $SHIV_{AD8}$ variants, recovered from three RP animals, were aligned with the starting $SHIV_{AD8}$ V3 loop. The V3 regions of the R5-tropic $SHIV_{SF162P3}$ and its $SHIV_{SF162\text{-}BR24N}$ derivative, which also emerged in an RP, are included in the alignment. (c) Coreceptor utilization of virus, pseudotyped with Envs present in RP DB99 at the time of necropsy, containing or lacking the 3-aa RIG V3 loop insertion.